

Experimental study of the Low Salinity effect using glass plate cell

Shell Rijswijk B.V.

Rijswijk, June 2012

COMPANY
PROFESSORS
COMMITTEE
CONTEXT

AUTHOR
SUPERVISORS

Shell Rijswijk B.V.
Ir. G. V. Woggelum & Dr. Ir. C. Swarts
Dr. Ir. A.W.F. Volker
Graduation thesis

Denis Ilic
Dr. H. Mahani & Dr. S. Berg

Preface

You are now reading a report that is written by Denis Ilic, a student of Applied Physics at the University of The Hague, Academy for Engineering.

This work is carried out at Shell Rijswijk B.V. between February 6 and June 1 2012 where laboratory research is done on the influence of brine salinity in model experiments. The project was a continuation on the previous work carried out by Elmer Jansen and Kirsten Bakker, while used methodology was completely renewed.

The work in this report is intended for Shell staff who are involved in the Low Salinity field and intend to get to the bottom of this field of research.

I would also like to make use of this opportunity to thank my supervisors Dr. S. Berg and Dr. H. Mahani for their tremendous help and support during my entire graduation process. Also would I like to thank all the people from the team who welcomed from day 1.

Denis Ilic

Rijswijk, May 2012

Summary

Laboratory research was done on flat glass substrates to study the effect that brine salinity has on adhesion mechanisms between oil and clay particles. This is done by evaporating a small clay suspension droplet (6 μl) on a glass slide that leaves a thin layer of clay upon which oil can be attached. When this glass slide is flooded under water, the oil that is attached to clay will form a droplet that can be investigated. It is expected that these droplets will detach when the salinity of the water is lowered. But the mechanism that is responsible for this detachment is still heavily debated and therefore not very well understood. To gain a microscopic perspective of the low salinity effect, the oil droplets have first been flooded in high saline brine (26,000 g/L totally dissolved solids, TDS) for two days so that the adhesion force and bouncy force get enough time to equilibrate. When the forces on the droplets equilibrated, the salinity of the brine was lowered to see how the droplets would respond to the low salinity water. This response is qualitatively measured by plotting the contact angle and contact area change of the droplets as a function of time. But before experiments were done in a controlled environment, the optimum experimental protocols were established first.

In a systematic study on the clay concentration it was found that the amount of clay in the suspension was a crucial factor whether the oil drops would respond to the low salinity. If the amount of clay in the suspension was too high (>250 mg/l for Montmorillonite), than the oil drops adhered too strongly to the clays and ultimately no sign of the low salinity effect would be observed. However, when the amount of clay in the suspension was too low (<100 mg/l for Montmorillonite), than the droplets would detach during the high salinity so the experiment had to be aborted.

The data from the new experimental methodology showed experimentally how exposure to low salinity water causes the oil to decrease its adhesion to the clay, and ultimately even detachment. The oil droplets presented in this study show a significant change in contact angle when they become exposed to low saline water, even when the uncertainty of 5 degrees is taken into account.

Caused by the experimental protocol, oil droplets varied in size (volume), initial contact area and initial contact angle. This variation gave additional experimental variables from the following observed general trends:

- (1) Droplets with larger volumes require less time to detach. That is indicative for the force balance acting on the contact area of the droplet: larger droplet volumes means larger buoyancy forces responsible for the detachment, i.e. larger buoyancy forces means shorter time to detachment.
- (2) An initially high contact angle (at start of LS), indicates stronger adhesion and as a consequence the detachment time is also relatively long.
- (3) When the initial contact area between the oil and clays, $A_{\text{contact area}}$, is high, then the detachment time of oil is long.

The third trend is interpreted as diffusion controlled equilibration of salt ions in the clay layer between the oil and glass substrate, which therefore critically influences the detachment kinetics of oil. The diffusion time scales were of the same order of magnitude as the experimentally observed detachment times. That supports the view that diffusion plays an important role in the detachment kinetics of oil.

Next, the detachment time was normalized by the diffusion time in order to account for contact area variation. The dimensionless time is defined as such that when it is plotted as function of salinity, it is inversely analogical to the oil production statistics found in the previous work. In the previous study the most oil production was found in the “controlled formation damage” section. Whereas in this study the lowest dimensionless time was observed in the “formation damage” section, meaning that formation damage (i.e. clay swelling) does not influence the oil detachment for the new methodology.

Table of Contents

Preface.....	1
Summary.....	3
Table of Contents.....	4
1. Introduction and basic concepts	6
1.1 Oil Reservoirs.....	6
1.2 Different types of rock	6
1.3 Porosity and Permeability	7
1.4 Improved Oil Recovery (IOR).....	8
1.5 Model system for representation of porous media.....	8
1.6 Forces acting on the oil droplets	9
1.7 Adhesion mechanisms	9
1.8 Wetting & contact angle	10
1.9 Clays and Double layers	11
2. Low Salinity flooding – literature review.....	13
3. Materials and methods.....	15
3.1 New method for attaching the oil to the glass slide.....	15
3.2 Importance of clay minerals in oil attachment.....	16
3.3 Schematic view of the experimental setup.....	17
3.4 The flow cell	18
3.5 Composition of the substances used in the	19
3.5.1 Brine (high and low salinity).....	19
3.5.2 Oil properties and background about the apparatus	20
3.5.3 Clay properties of the used clays	20
3.6 Method for measuring the contact angle and contact diameter.....	22
4. Materials and methods.....	24
4.1 Overview of the experiments.....	24
4.2 Determining the optimum clay patch size vs. clay concentration (for Montmorillonite)	25
4.1.1 Influence of clay patch shape	26
4.3 Experimental approach	27
4.4 Experimental results exhibiting the Low Salinity effect	28
4.5 Is the process controlled by diffusion?	34
4.5.1 Dimensionless parameters.....	37
4.3.2 Additional normalization attempts.....	39
5. Conclusions.....	41
6. References.....	43

Appendix 1. Oil and brine properties.....	44
Appendix 2. Further investigation of clay concentrations	46
Appendix 3. Overview of the experiments	52

1. Introduction and basic concepts

In this chapter a short explanation of oil reservoirs, rock types, adhesion mechanisms and clays will be given. In section 1.5 the representativeness of the used experimental is explained by illustrating the way oil is clustered in a reservoir, and how this relates to the model experiments.

1.1 Oil Reservoirs

The crude oil that is found in oil reservoirs is formed in the Earth's crust over a period of millions of years. Various evidence and models indicate that oil is the result of compressing the remains of living things under a thick layer of sand or rock. In summary, an oil producing reservoir needs the following:

- Porous and permeable reservoir rock
- Source rock supplying hydrocarbon
- Trap rock that prevents the oil to escape from the reservoir

In Figure 1.1 a typical cross section of an oil reservoir is presented.

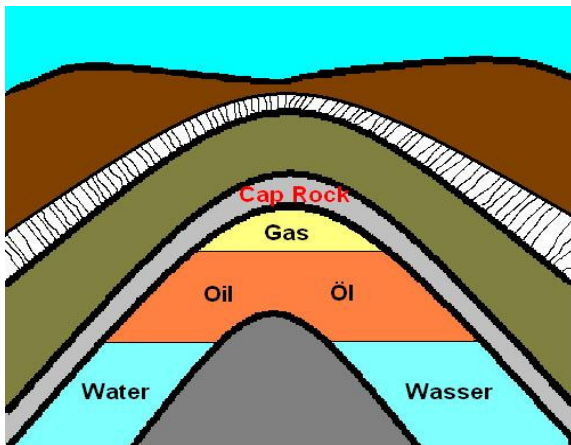


Figure 1.1: Typical cross section of an oil reservoir. This form is often called an anticline. [10]

1.2 Different types of rock

Reservoir rocks are dominantly sedimentary (sandstones and carbonates). Sandstone rock comprises mostly of quartz grains, and/or feldspar, and is surrounded by void spaces that can contain substances like water, gas or oil. The grains are typically coated with clay minerals (which are further described in section 1.7) and play an important role in wettability state of rock. The void spaces, also known as pores, can migrate these substances if they are connected.

Carbonate rocks are on the other hand primarily composed of carbonate minerals of which limestone and dolostone are the most common. Limestone is composed out of calcite and aragonite (different crystal forms of CaCO_3), and dolostone is composed of the mineral dolomite ($\text{CaMg}(\text{CO}_3)_2$). The minerals in these carbonates seem to play a significant role in the Low Salinity effect according to some scientific research [2]. The way in which these minerals seem to play a role will be discussed in section 1.7.

1.3 Porosity and Permeability

Porosity is the measure of the void space in a material, in this case a rock. Every rock, or some other material for that matter, has a bulk volume, and a volume of void space. This volume of void space divided by the bulk volume is what is defined as the porosity and is always a number between 0-1. But one could also define a certain volume of grains. The porosity is then defined by equation 1.1.

$$\phi = \frac{V_b - V_g}{V_b} = \frac{V_p}{V_b} \quad (1.1)$$

Where: ϕ is the porosity [-]

V_b is the bulk volume [m³]

V_p is the void space [m³]

V_g is the volume of the grains [m³]

Permeability on the other hand, is the ability of a rock to pass a fluid through its porous media. One of the first people who researched this field was Henry Darcy. He discovered for example that the flow rate q , is proportional to the area A of the cross section and the applied pressure difference ΔP , while the flow rate is also inversely proportional to fluid viscosity μ and the length L of the system. With this knowledge the following equation can be written:

$$q = \frac{k \cdot A \cdot \Delta P}{\mu \cdot L} \quad (1.2)$$

Where: q is the flow rate [m³/s]

A is the area of the cross section [m²]

ΔP is the applied pressure difference [Pa]

μ is the fluid viscosity [kg/m·s]

L is the length or the thickness of the bed of the porous medium [m]

k is the proportionality constant [m²]

This proportionality constant k is what is known as the *permeability*. The official SI unit is in m², but the traditional unit is the *darcy* (D), or even more commonly the *millidarcy* (mD). 1 darcy is approximately equal to 10⁻¹² m².

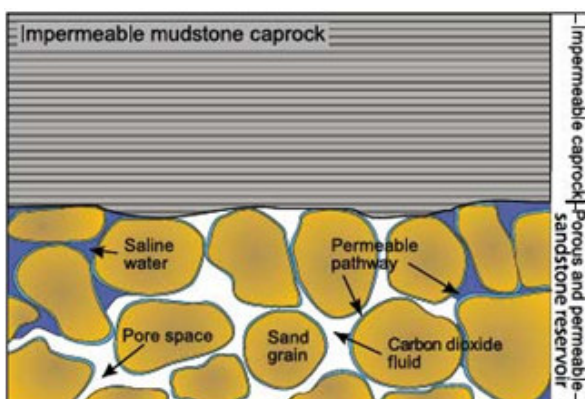


Figure 1.1: Illustration of porosity and permeability within a sandstone reservoir. [3]

Figure 1.1 illustrates how a possible oil reservoir looks on a microscopic scale. The pore spaces are relatively large and good interconnected so that oil and water (or in this case CO₂) can migrate

without much resistance. The figure also shows the third basic requirement for an oil producing reservoir: the impermeable caprock that prevents the oil to “ escape” due to the high pressure in the ground that builds up over a period of millions of years. It is believed that a lot more oil would be in the ground today, if only at some places there would have been a caprock.

1.4 Improved Oil Recovery (IOR)

When the primary oil recovery of a reservoir is exhausted, one can do two things: abandon the oil reservoir, or use secondary methods to force the remaining oil to the surface. Secondary oil recovery or improved oil recovery (IOR), are methods in which the high pressure of the reservoir is maintained in order to extract the remaining oil out of the reservoir. This is done by water and gas injection.

The water that is injected to maintain the pressure of the reservoir is injected underneath the oil. Because water is denser than oil, the oil floats on top of the water and eventually pushed to the production well.

1.5 Model system for representation of porous media

When an oil reservoir is depleted during primary and secondary oil recovery, it goes through three stages. Initially, the oil in the pore scale of the reservoir rock is interconnected and therefore easily extracted. When the natural pressure of the reservoir decreases, waterflooding is used to maintain the pressure and displace the oil. At this stage, some portions of the oil is not interconnected anymore but attached as a cluster or single drops to the clay (marked red in Figure 1.2) of the individual grains, see Figure 1.2b. When eventually the salinity of the water is decreased, the working hypothesis is that some of the oil-clay contacts are weakened and break which leads to the additional oil recovery, see Figure 1.2c.

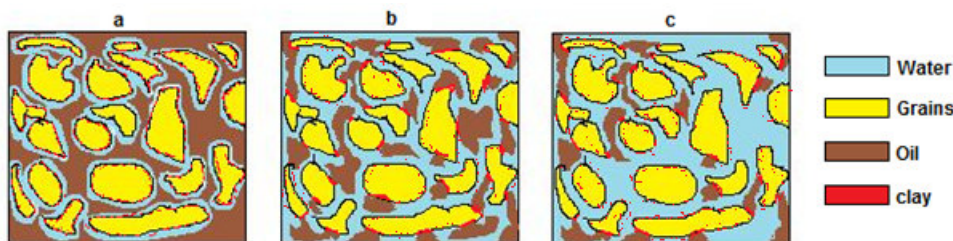


Figure 1.2: Illustration of the three stages of an oil reservoir during primary and secondary oil recovery. Figure (a) is the initial stage, figure (b) is after regular water flood and figure (c) is after low salinity water flood. Note how in figure a the yellow grains are surrounded by water and the oil at the pore scale is interconnected. In figure a and b this is clearly not the case anymore.

The working hypothesis is now tested in a simplified model system. By investigating the way how oil is detached from the clay in a controlled environment (explained in section 3), it is possible to get a better and fundamental understanding of the processes that play in the low salinity effect. The oil that remained attached to the clay in Figure 1.2 can be illustrated as in Figure 1.3.

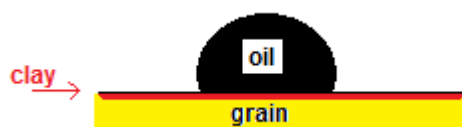


Figure 1.3: Model system: illustration of the way oil is attached to the clay in a pore.

1.6 Forces acting on the oil droplets

There are two main forces that act on an oil droplet when it is submerged under water: The adhesion force between the clays that points downward, and the buoyancy force that is pointed upward because oil is less dense than water.

This buoyancy force can be explained by Archimedes' principle, which states: "Any object immersed in a fluid, is buoyed up by a force equal to the weight of the fluid displaced by the object". Therefore the density of an object decides whether it will sink or float. It was already mentioned that oil has a less density than water, so when it is submerged in water the buoyant force is given by:

$$F_b = \rho_{\text{brine}} \cdot V_{\text{displaced}} \cdot g \quad 1.3$$

So the net upward force is:

$$\begin{aligned} F_{\text{upward}} &= F_b - F_g \\ F_{\text{upward}} &= \rho_{\text{brine}} \cdot V_{\text{displaced}} \cdot g - \rho_{\text{oil}} \cdot V_{\text{oil}} \cdot g \end{aligned} \quad 1.4$$

Since the volume of displaced brine equals to the volume of the oil, for the upward force also can be written:

$$F_{\text{upward}} = (\rho_{\text{brine}} - \rho_{\text{oil}}) \cdot V_{\text{oil}} \cdot g \quad 1.5$$

All brine and oil densities are listed in APPENDIX 1.

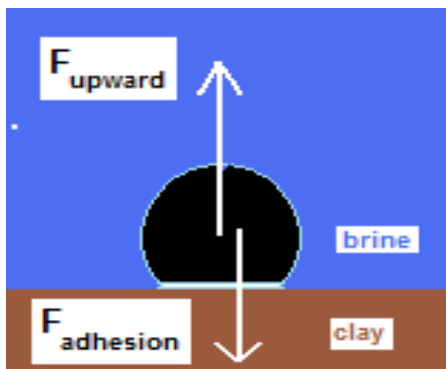


Figure 1.3: Forces that act on the droplet.

On the other hand, the adhesion force that is pointed downward is proportional to the contact area between the oil and clay. And this contact area is in turn proportional to the contact angle the droplet makes with the clay, measured from the brine side because it is the more dense fluid. In section 1.8 this notion will be further explained.

1.7 Adhesion mechanisms

The forces that are responsible for these effects can be divided into several categories: chemical adhesion, dispersive adhesion, electrostatic adhesion and diffusive adhesion.

Chemical adhesion occurs when the surface atoms of two separate surfaces form ionic, covalent or hydrogen bonds. However, covalent bonding is more a chemical interaction, while ionic, hydrogen and van der Waals bonds are more associated with adhesion. These bonds however, will only occur if these surfaces have the opposite charge, otherwise they will repel. Note that chemical adhesion only

plays a role if these surfaces are very close to each other, because ionic and hydrogen bonds are only effective over very small distances (<1 nm). In this work surface forces are treated only as effective forces expressed as surface energy accessible by macroscopic measurements of contact angle.

1.8 Wetting & contact angle

The wettability of a liquid is its ability to maintain contact with a solid surface, resulting from intermolecular interaction. On plane surfaces, the degree of wetting is measured by the contact angle.

When a water droplet is on a leaf or a table, the situation as in Figure 1.4 can be sketched. The contact angle is the angle at which the liquid-vapor interface meets the solid interface. But in the case of water and oil, the contact angle is determined through the water phase because water is the denser fluid, see Figure 1.4 and 1.5.

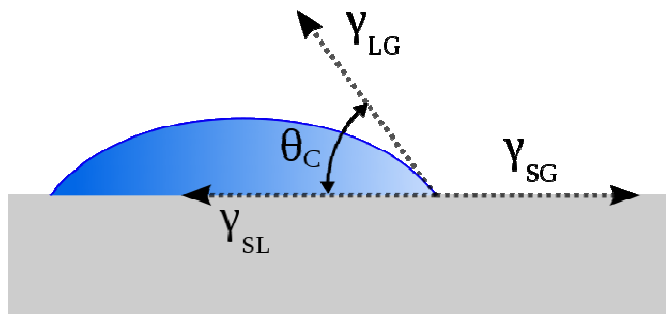


Figure 1.4: Contact angle between water, air and some unknown solid surface. [10]

By adding the horizontal component of the interfacial tension between the liquid and air, γ_{LG} , to the already horizontal interfacial tension between the solid and the liquid, in a static case one can write down the following force balance on the 3-phase contact line:

$$\gamma_{SG} = \gamma_{SL} + \gamma_{LG} \cdot \cos \theta_C \quad 1.6$$

Where: γ_{SG} is the interfacial tension between the solid and gas (in this case air)

γ_{SL} is the interfacial tension between the solid and liquid (in this case water)

γ_{LG} is the interfacial tension between the liquid and gas

There are two main types of solid surfaces that liquids can interact with. These two types of surfaces are divided into high energy and low energy solids. The energy of a solid depends on the nature of the solid itself. Solids such as metals, glasses ceramics and rock minerals are known as hard solids, for the chemical bonds that hold them together are usually very strong (covalent, ionic or metallic bonds). On the hand the solids that are being held together by much weaker forces (Van der Waals forces or hydrogen bonds), are therefore called low energy solids because it requires less energy to break those bonds. Depending on the type of liquid, low energy surfaces permit partial or even complete wetness, whereas high energy surfaces wet completely most of the time. [4]

In Figure 1.5 it is illustrated that if the contact angle is large, the wetting between the oil and the clay minerals is strong with the result that the oil spreads over the surface. On the other hand, when the contact angle is small, the oil will form a drop, hence the surface is called *water wet*. The wetness of a surface can be described as result of certain types of surface tension. In Figure 1.5 below, the vectors γ_{so} , γ_{sw} and γ_{ow} are drawn, in which γ_{so} represents the surface tension between the surface and the oil, the vector γ_{sw} represents the surface tension between the surface and water and γ_{ow} represents the

surface tension between oil and water. Whether the surface tension between the clay minerals (surface) and the oil is high or low, depends on the intermolecular interaction between the two.

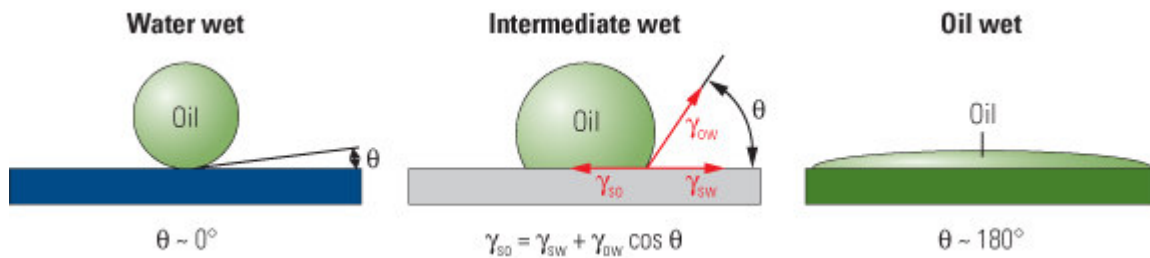


Figure 1.5: Different forms of wettability shown between water-oil-clay interactions. Note how the contact angle is measured from the opposite side compared with figure 1.4. Contact angle is always measured from the denser fluid. [5]

This more water wet situation as it is represented in Figure 1.5, is much more preferable than the oil wet one. Because a high degree of oil wetness means that the oil is much stronger attached to the rock or surface, which is unfavorable for oil recovery. So by changing the wettability to more water wet, oil recovery can be improved.

1.9 Clays and Double layers

Because the crystal lattice of clays are submitted to imperfections, their top faces are usually negatively charged. Just as the clays, oil molecules also usually have a charge. This charge can either be positive or negative. To find out what the net charge of an oil sample is very complex and not in the line of work presented in this report. But for the attachment of oil to clays, it does not matter whether the polar component in oil is positive or negative, see Figure 1.6a.

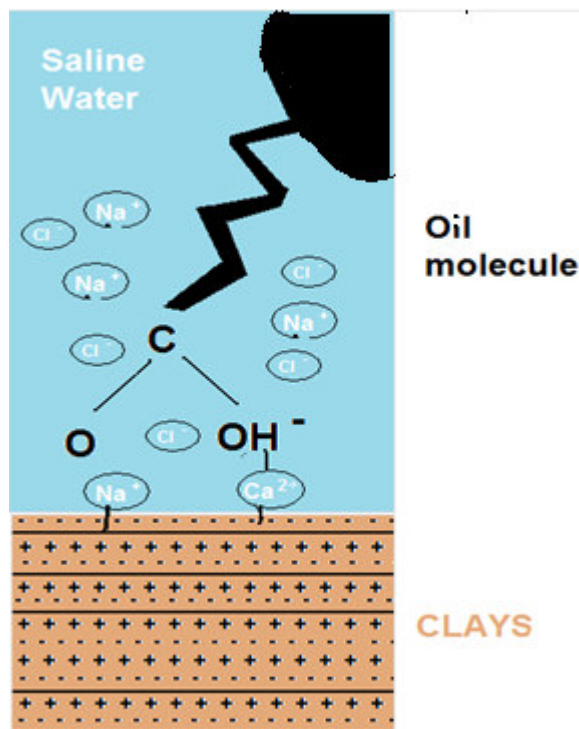


Figure 1.6a: Illustration of the binding between clays and oil

The attachment between oil and clay, i.e. adhesion force, can be explained by so called *electric double layers*. When particles are brought together within a short distance, they are attracted to one another by the van der Waals force. But nevertheless, the dissolved salts are due to Brownian motion able to move freely within the brine. These salts have the quality to (homogeneously) disperse in such a way, so that charges are compensated and free enthalpy is minimized [6]. The negatively charged clay layer will therefore attract positively charged ions such as Na^+ and K^+ to become electrostatic neutral and pursue minimal energy. The dissolved salts are therefore no longer homogeneously distributed because there are now more cations near the clay surface than in the rest of the brine. The negatively charged clay and positively charged ions now form an electric double layer, see Figure 1.6 below.

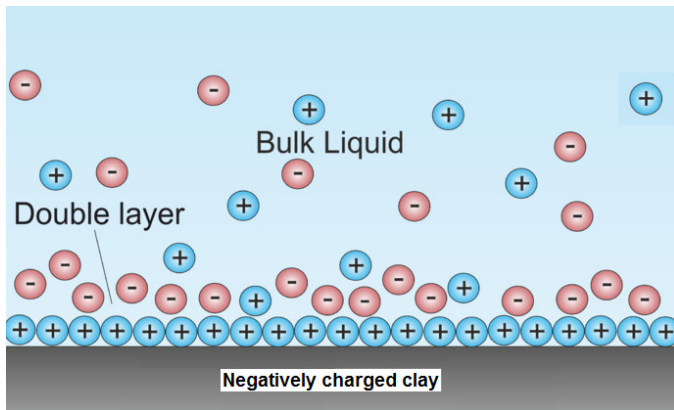


Figure 1.6b: Negatively charged clay layer attracts cations, thus forming an electrochemical double layer. [22]

Stronger attachment between oil and clay is possible when divalent cations such as Mg^{2+} and Ca^{2+} are also present in the brine. It is argued that these divalent cations form bridges between the negatively charged clay particles and negative oil components. When the system is flooded with lower saline brine, the cations in the double layer tend to exchange with other incoming ions and diffuse to maintain maximum entropy of the system. This effect is believed to seize these bridges and thus decreasing the adhesion force between oil and clay, which in turn makes the droplet more oil-wet and eventually even detach.

2. Low Salinity flooding – literature review

Primary oil recovery techniques are no longer sufficient because they leave relatively large amounts of oil behind in the reservoirs. When an oil field is recovered with the primary method, the natural high pressure of the field is usually enough to push the oil towards production well. Over time, the pressure of the well decreases and primary oil recovery eventually stops. Improved oil recovery techniques, i.e. waterflooding (via water injection), are then executed to displace the remaining oil and maintain pressure of the oil field.

For waterflooding typically, reservoir salinity is used to stabilize the clay minerals and hence avoid formation damage as a result of clay swelling. The salinity of water found in reservoirs is usually very high compared to the water that is found at the surface. But nevertheless, it has been discovered [7] that by lowering the salinity of the water, oil recovery can be improved by 5-10%. Since then this phenomenon has been studied by many researchers and is currently being applied in the field.

This additional oil recovery can on a macroscopic scale be parameterized as the effective wettability modification to a more water-wet state. This change in wettability from oil-wet to water-wet is highly preferable due to a decrease in bonding between oil and clays. Apart from the understanding that low salinity water is capable of changing the contact angle to a more water-wet state, there is still much debate going on about what is happening on a microscopic scale. An experiment [7] showed that the low salinity effect occurs on sandstone rocks, but does not in fired or acidized sandstones. Based on this finding Tang and Morrow concluded that the effect is related to the presence of clay minerals. Upon this conclusion, a couple of well received proposals have been made by other researchers in the field:

1. Multicomponent ion exchange mechanism [8],[9],[10]: In this mechanism the polar components in the oil phase are adsorbed to the clay surface through ion binding with divalent ions in the water phase. The low salinity water is believed to act in such a way that the double layer expands and enables the divalent ions, and its associated oil components, to exchange with the incoming ions. See section 1.9.

2. Formation damage mechanisms: Although formation damage (i.e. migration of fines and clay minerals with the consequence that the permeability of the rock decreases) in the reservoir used to be undesirable and was therefore avoided as much as possible, nevertheless some researchers believe this could be the fundamental reason behind improving oil production with low salinity water. Because experiments [11] showed that in presence of high saline brine clays become more stable, while low saline brine makes the clays swell. It is therefore argued that only the pores that contain (low saline) brine will swell, leaving the pores that contain oil as they are. And it is this effect that is believed to be responsible for the extra release of oil. Because in this way all the flow will be directed to pores that contain oil, skipping the pores that only contain brine. Nevertheless, during numerous low saline, reservoir conditioned core flood experiments [12], which all have shown increased oil recovery, no fines migration or permeability reduction were observed. These findings opened up the discussion whether fines migration really does play a significant role in the low salinity effect.

3. pH increase: Since it was reported [13] that additional oil recovery is accompanied by a pH increase to about 8, it was suggested that this is due to a combination of ion exchange and carbonate dissolution/release. Later, Austad [14] proposed a chemical mechanism that was based on the sudden decline of divalent cations, hence low salinity flooding, which ultimately leads to a “local” increase in pH and therefore desorption of adsorbed polar oil components. Nevertheless, Lager states [8] that increased pH induced recovery cannot be the mechanism behind the low salinity effect because an increase in pH has not been observed in all low salinity studies.

In this work an attempt is made to gain further insight into low salinity mechanism by designing and executing experiments using a model system described earlier in section 1.5. The material and methods are explained in the section 3. The results of the experiments are presented in section 4 and conclusions and recommendations are given in the section 5.

3. Materials and methods

While the previous work [15] only focused on the oil production that is accomplished with the low salinity effect, this work is a quantification of contact angle and contact area changes. In the experimental set up used by the previous students this was not possible because the glass slides were covered with a relative big amount of clay, which in turn swelled up a lot when it was flooded with low salinity water. Due to this large swelling it was therefore impossible to make decent estimates about contact angle changes. With the new developed method of attaching the oil to the clay, contact angle measurements are feasible.

With this new method a series of experiments have been conducted in order to gain a better understanding of the different aspects of the low salinity effect. It was already mentioned that the previous set up by had some experimental drawbacks that were hard to overcome. For instance, it was not possible to produce oil droplets on the substrate that roughly had the same volume. Another issue had to do with the large amount of clay that covered the glass using glue. One cannot be entirely sure what kind of role the glue plays in the interaction between clay and oil. With the new experimental method that is described in section 3.1, all of the just described issues are solved. On Elmer's and Kirsten's previous work the emphasis was mainly on oil production statistics. Whereas in this report the main emphasis will be laid on the contact angle changes (i.e. adhesion decrease), and how this relates to the brine composition. In the following chapter a basic outline of the used experimental methods will be given that helped researching all these aspects of the low salinity effect.

3.1 New method for attaching the oil to the glass slide

Before starting the experiment, the glass [16] was cleaned to avoid any contamination. The glassware is cleaned with a Hellmanex® solution, which is a mixture of alkaline and surfactants. These alkaline surfactants are completely removable when flushed with sufficient water. The experimental protocol for cleaning has the following steps:

- Wash the beakers and glass slides off with milliQ-water or demiwat. Then fill a big beaker with (demi)water and add the Hellmanex® according to the description, and put the glassware in the beaker containing the Hellmanex® solution.
- Put the beaker with all its glassware and Hellmanex® solution in an ultrasonic bath for at least 60 minutes on a temperature of 50°C.
- After the ultrasonic bath, take the beaker out and wash all the glassware off with plenty of demiwat until all the Hellmanex® surfactants are gone and let the glass slides dry in a vacuum chamber. This is because if the glass dries in a atmospheric environment, it will after a while not be completely clean anymore due to air contact.

When the glass is dry, a number of small clay patches are placed on the glass. This is done by making a clay suspension and using a pipette. With the pipette a very small droplet of the clay suspension is applied on to the glass, as shown in Figure 3.1a. When these droplets are evaporated, a small and thin clay patch will remain because clay naturally adheres to the glass, see figure 3.1b. The next step is then to attach the desired oil amount on to the clay substrate. For the experiments described in this report the oil amount was varied from 2 μl up to 35 μl , and the clay concentration was varied from 100 mg/l to 500 mg/l. The results of these experiments are documented in the next chapter.



Figure 3.1a: 8 clay suspension droplets, each has a volume of $6 \mu\text{l}$

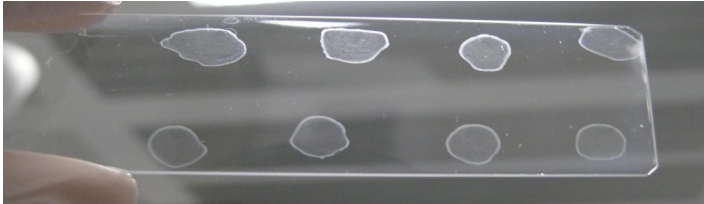


Figure 3.1b: clay substrate on which the oil attaches, after the water from the clay suspension is evaporated

3.2 Importance of clay minerals in oil attachment

In Figure 3.2a oil is placed on a glass slide that did not contain clay patches, and then placed in high saline brine so oil droplets would form. After only three seconds all the droplets matured, and after 76 seconds almost all detached, see Figures 3.2b and 3.2d.

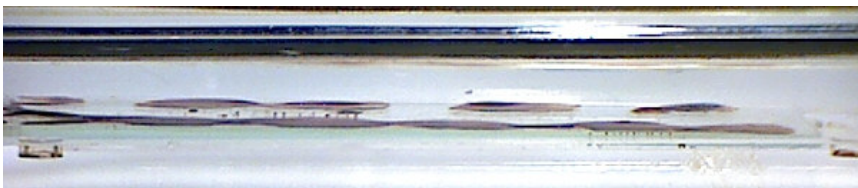


Figure 3.2a: The first second of flooded oil droplets on a clean glass slide that did not contain clay. $t = 0\text{s}$

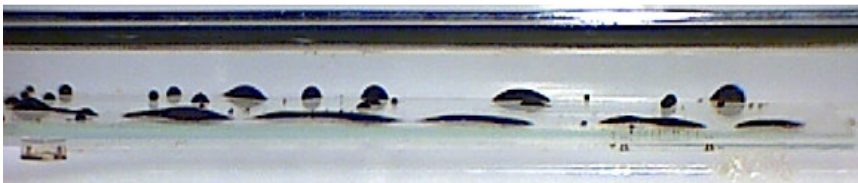


Figure 3.2b: Start of the formation of matured droplets on $t = 3\text{s}$

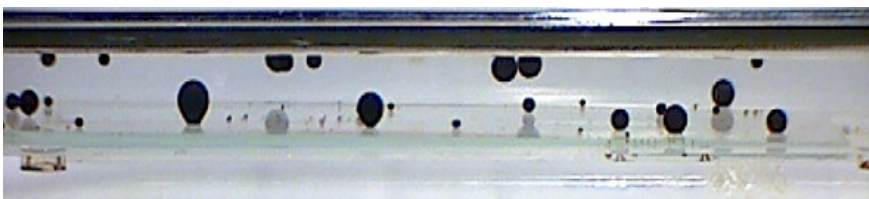


Figure 3.2c: After 20 seconds half of the droplets detached, and the remaining droplets are in the process of detaching.



Figure 3.2d: After only 76 seconds 90% of the oil droplets detached from clean glass.

Where in Figure 3.2 oil is placed on regular glass slide without clay on it, in figure 3.3 the situation is shown when the oil is placed on dried clay patches. Figure 3.3a shows the initial stage at $t=0$ when the glass slide is placed in the high saline brine. Figures 3.3b to Figure 3.3d illustrates how the droplets remain attached to the clay, in contrast to the situation when there is no clay placed on the glass (Figure 3.2).



Figure 3.3a: : Illustration at the start of attached oil droplets on clay substrates after $t = 0s$.

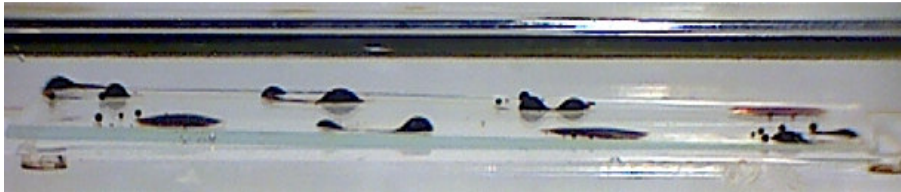


Figure 3.3b: Illustration of the attached oil droplets on clay substrates after $t = 12s$.

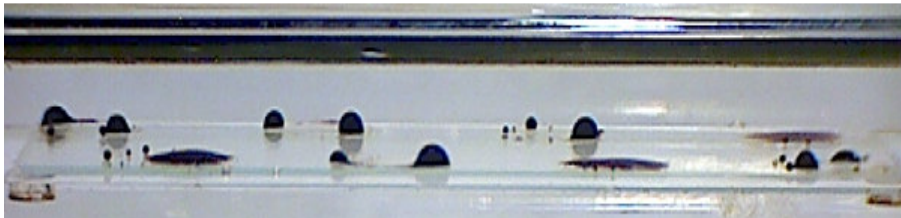


Figure 3.3c: Illustration of the attached oil droplets on clay substrates after $t = 180s$

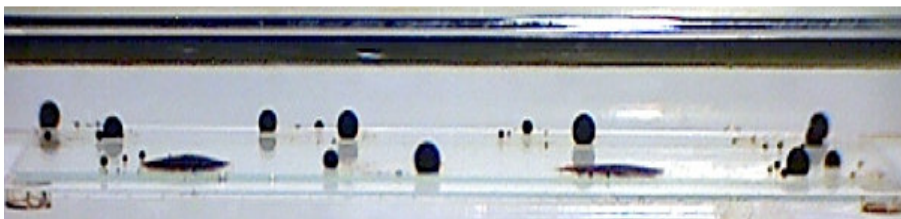


Figure 3.3d: Illustration of the attached oil droplets on clay substrates after $t = 3,5h$

These tests indicate that clay plays an important role in anchoring oil droplets to glass slide. A similar effect can be expected in porous media saturated with oil where in clean quartz grains (composing matrix of sandstones) do not naturally tend to bind oil. In other words clean quartz grains in absence of clay mineral are water-wet. Therefore there is no scope to apply low salinity flooding to recover oil via the mechanism described earlier, as those mechanisms involve clays.

3.3 Schematic view of the experimental setup

It was already briefly mentioned in the introduction, that the experimental setup that was used in this study is somewhat different than the set up used in the previous project ([15] Cense, Berg, Jansen, & Bakker, 2011). In the previous project a pump was used to create a constant flow rate in the flow cell. In order to make the water flow, the gravity (i.e. height of the water level) is used. After some period of time the water level in the tank would drop, and hence decrease the flow rate. To prevent this, the water that flowed out of the flow cell, was pumped back into the reservoir to maintain the water level and keep the flow rate constant, see Figure 3.3.

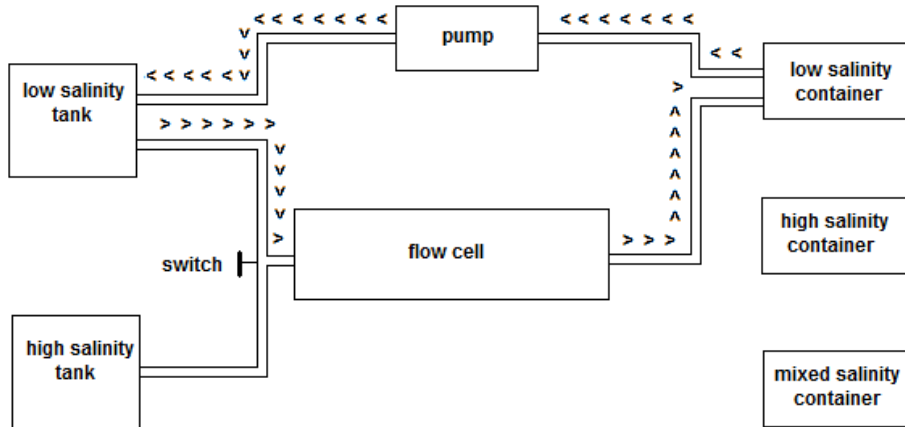


Figure 3.3: schematic drawing of the previous set up by Elmer Jansen and Kirsten Bakker

The pump from Figure 3.1 is removed, because in the experiments it was not required to have permanent flow. So the set up from Figure 3.3 can be simplified according to Figure 3.4. It is also important to note that the clays were not attached to the glass with glue, in contrast to the experiments performed in the previous work [15]. The effect that these glue molecules had on the oil-clay interaction wasn't entirely known, which is the main reason why the glue is avoided for this study.

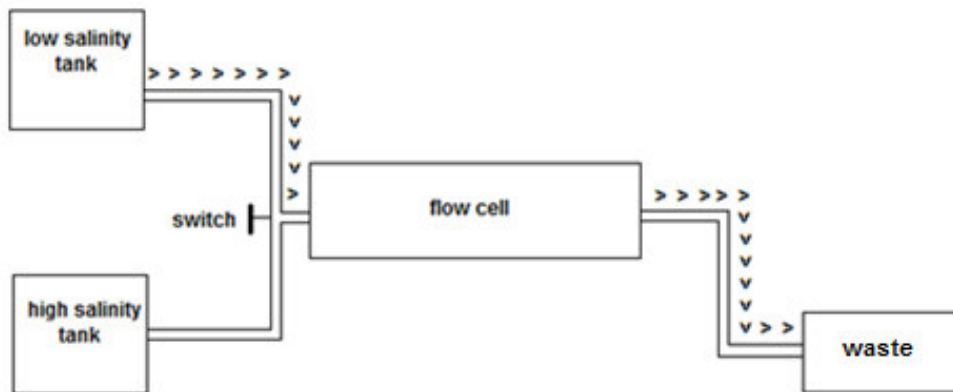


Figure 3.4: schematic drawing of the set up used in this report

3.4 The flow cell

The flow cell that was used for the experiments is sketched in Figure 3.5. The flow cell is a custom in-house design and built by Shell. The bottom half of the flow cell is made of Perspex in which there is a hollow flow chamber. The dimensions of the flow chamber are 120 mm by 40 mm by 10 mm. A compartment is made to accommodate the glass slide which has the dimensions 76,5 mm by 25,5 mm by 1 mm. The flow chamber has an inlet with a diameter of 8 mm and an outlet of 4 mm which are both connected to tubes which in turn are connected to high or low salinity tanks.

The upper part of the flow cell is a straight piece of Perspex to close the flow space. In between the upper and lower part of the cell, there is an O-ring to prevent possible leakage. Four bolts and nuts are used to press the lower and upper parts together.

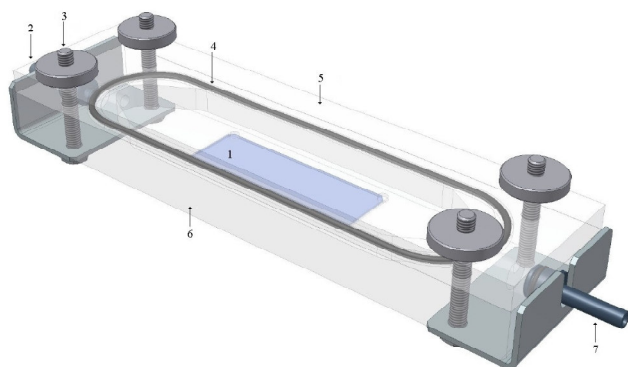


Figure 3.5: sketched image of the used flow cell. 1) glass slide; 2) inlet; 3) screw bolt; 4) rubber O-ring; 5) upper part of the flow cell; 6) bottom of the flow cell; 7) outlet. [17]

3.5 Composition of the substances used in the

In this paragraph the composition and properties of all the substances used during the experiments will be given. For example high and low saline brine composition, oil properties, structure of the used clay minerals etc. Also in appendix 1 the densities of all the used fluids can be found as a function of temperature.

3.5.1 Brine (high and low salinity)

Brine is water with a certain concentration of salt. The high saline brine that was used during the experiments is also called Morrow brine (MB) [7]. Table 1 shows the composition.

Table 3.1: Morrow brine composition

Substance	Concentration [g/l]
NaCl [g/l]	10,85
KCl [g/l]	13,80
CaCl ₂ ·2H ₂ O [g/l]	1,106
MgCl ₂ ·6H ₂ O [g/l]	0,194

The divalent cations Ca²⁺ and Mg²⁺ are put into the composition to see how the oil-clay attachment corresponds to a case when the oils and clays are not put into water that has these divalent cations.

When the oil droplets that are attached to the clay patches are flooded with high saline water and have equilibrated, then the water in the flow chamber is replaced by low saline water. This is done by letting approximately 1 liter low saline brine flow into the flow chamber. Since the volume of the flow chamber is 0,050 dm³, this means that the high saline brine is mixed with 20 times its original volume. The low saline water that was used during the first experiments was 8x diluted Morrow brine. Later, also experiments were done for 4x and 16x diluted Morrow brine.

Finally, a series of compositions are made that only contained regular NaCl. As just is briefly mentioned, this is done to see what the effect will be on the rate of contact angle change and oil detachment when there is an absence of divalent cations in the brine. The salinity of water that only contained NaCl had approximately the same amount of *total dissolved solids* (TDS) as the low saline Morrow brine counterparts so that valid comparisons could be made. See Table 3.2.

Table 3.2: Used brine compositions

Brine	NaCl (g/l)	KCl (g/l)	CaCl ₂ ·2H ₂ O (g/l)	MgCl ₂ ·6H ₂ O (g/l)	TDS
Morrow brine	10,85	13,80	1,106	0,194	26000
4x diluted Morrow brine	2,713	3,450	0,2765	0,0485	6500
8x diluted Morrow brine	1,356	1,725	0,1383	0,02425	3250
16x diluted Morrow brine	0,6781	0,8625	0,0691	0,01213	1625
low saline NaCl #1	6,500	[-]	[-]	[-]	6500
low saline NaCl #2	3,250	[-]	[-]	[-]	3250
low saline NaCl #3	1,625	[-]	[-]	[-]	1625

3.5.2 Oil properties and background about the apparatus

The oil that was used in the experiments is Brent bravo crude. Its average density at 23°C is 0,844 g/cm³ and its average (dynamic) viscosity is 6,5378 mPa·s. At a temperature of 30°C the average density and viscosity are sequentially 0,839 g/cm³ and 5,2785 mPa·s. properties are measured with an apparatus that can measure density and viscosity at any desired temperature. The apparatus is an Anton Paar SVM 3000 / G2, see Figure 3.6.



Figure 3.6: Representation of the Anton Paar SVM 3000 / G2 apparatus.

Within in a range of 0,65 – 1,5 g/cm³ the error is ±0,0005 g/cm³ and ±0,0020 outside this range. As for the viscosity the margin of error is always ±0,35% of the initial measured value. In appendix 1 more properties of the used fluids are documented.

3.5.3 Clay properties of the used clays

In this report two types of clays have been used: Na-Montmorillonite (Wyoming) SWy-1(SWy-2) and Kaolinite KGa-2, of which only Montmorillonite was used for controlled experiments. These clays have been supplied by the Clay Mineral Society [18]. In this section the properties of these clays will be briefly discussed.

Montmorillonite

The Montmorillonite clays are from the County of Crook, State of Wyoming, USA. The chemical composition is shown in table 3.3. Furthermore, the Cation Exchange Capacity (CEC) is 76,4 meq/100g. The CEC is the maximum quantity of total cations that a soil or clay is capable of holding, at a given pH value, available for exchange with the soil solution.

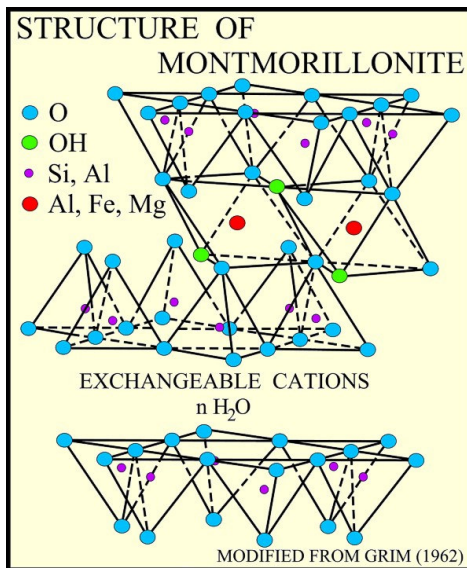


Figure 3.7: Structure of the Montmorillonite clay [18]

Table 3.3: Chemical composition of Montmorillonite clay

Molecule	Composition [%]	Molecule	Composition [%]
SiO ₂	62,9	CaO	1,68
Al ₂ O ₃	19,6	Na ₂ O	1,53
TiO ₂	0,090	K ₂ O	0,53
Fe ₂ O ₃	3,35	F	0,111
FeO	0,32	P ₂ O ₅	0,049
MnO	0,006	S	0,05
MgO	3,05		

Kaolinite

The Kaolinite clays are from the County of Warren, State of Georgia, USA. The chemical composition is shown in Table 3.4 and the CEC is 3,3 meq/100g, which is significantly less than Montmorillonite. This explains also why Kaolinite is known as a clay that swells significantly less in comparison with for instance Montmorillonite.

Table 3.3: Chemical composition of Kaolinite clay

Molecule	Composition [%]	Molecule	Composition [%]
SiO ₂	43,9	MgO	0,03
Al ₂ O ₃	38,5	Na ₂ O	<0,005
TiO ₂	2,080	K ₂ O	0,065
Fe ₂ O ₃	0,98	P ₂ O ₅	0,045
FeO	0,15	S	0,02

For more information about the used clays, see source [18].

3.6 Method for measuring the contact angle and contact diameter

When the oil is attached to the clay patch and flooded with high saline brine, it usually goes from an initial-predominant oil-wet state to a somewhat water-wet state, see Figure 3.7 and 3.8.

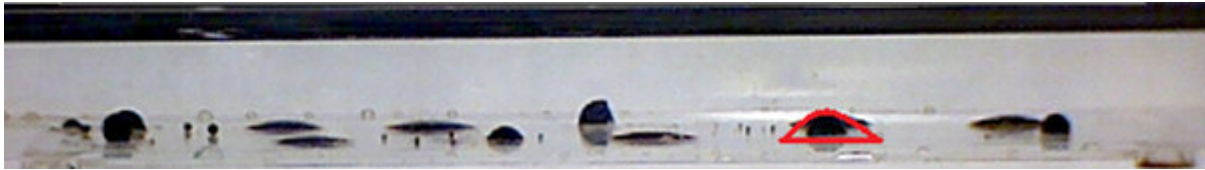


Figure 3.7: The initial oil-wet state at the beginning of exposure to high salinity water. The contact angle of the droplet that is hatched in red will be in figure 3.10, 3.11 and 3.12 further analyzed.



Figure 3.8: the end of approximately two days exposure to high. Note how the contact angle of the droplets changed from oil-wet to more water-wet.

This change from oil-wetness to more water-wetness stops when an equilibrium is reached. When the oil is exposed to high saline brine for a few days, and no oil droplets have detached and a stop of contact angle change is observed, one could say the upward and downward forces (buoyancy, adhesion) on the oil droplets have equilibrated. When this equilibrium is reached, a switch to low salinity water is made. When exposed to low salinity water, the contact angle will continue to change over time and go towards a more water-wet state. This change in contact angle is measured and then plotted in an Excel spreadsheet, which can be found in the next chapter. Figure 3.9 typically shows how a droplet detaches when exposed to low salinity.

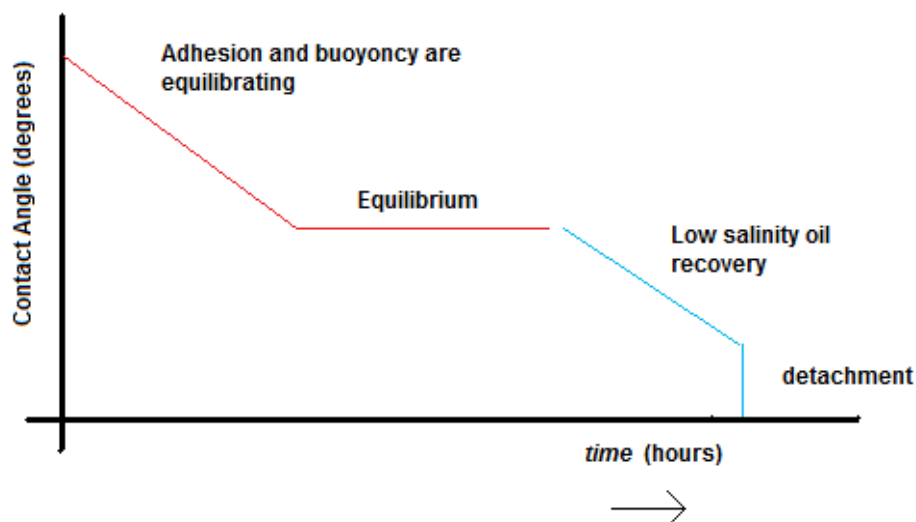


Figure 3.9: Illustration of a typical oil detachment process measured by the change in contact angle vs. time.

This contact angle change is measured as a function of time with an angle-measurement tool from ImageJ. When the desired snapshot is uploaded to ImageJ, the snapshot is zoomed in to area where the oil makes contact with the clay and the water, see figure 3.10. The contact angle is measured through the water phase. To determine the error in contact angle, again the angle measurement tool from ImageJ is used, see Figures 3.11 and 3.12.



Figure 3.10: estimation of the contact angle, measured with the zoom and angle-measurement tool from ImageJ.



Figure 3.11: determination of the error margin on the left side of the contact angle

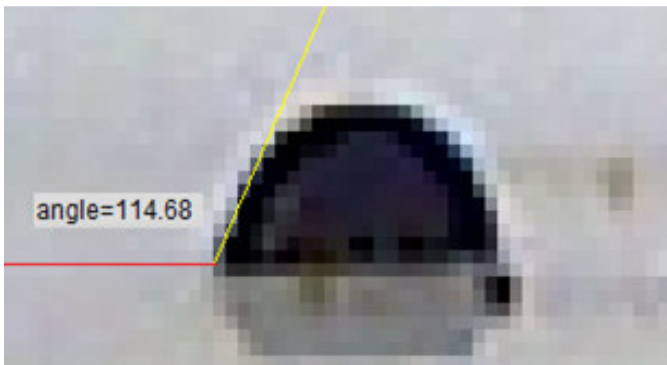


Figure 3.12: determination of the error margin on the right side of the contact angle.

The contact angle is measured as a function of time for every droplet and every experiments that showed a positive reaction the low saline water. In section 4.2 the definition of “a positive reaction to low saline water” will be given.

In addition, measuring the diameter of the contact area was done by calibrating the ‘measure tool’ of ImageJ with the known length of the glass slide. Because the length of the glass slide was known up to two digits after the comma (in mm), also the diameter of the contact area could be measured very accurately, if at least the resolution of the images was clear.

4. Materials and methods

In this chapter the results of the performed experiments will be presented, which includes the following:

- An experimental approach and overview of the experiments
- Results for determining the optimal clay patch size and clay concentration
- Experimental results Low Salinity effect
- Results of the normalized data and diffusion times

4.1 Overview of the experiments

Over a period of 17 weeks, roughly 34 experiments have been conducted, see Table 4.1. Table 4.1 shows a summary of the performed experiments that have been done. It tells how much time each experiment took and what the average contact angle change during high salinity and low salinity was. Although experiment #34 responded positively to the low saline water, unfortunately there wasn't enough time to include that data in this report.

Table 4.1: Overview of the experiments

Exp #	Low sal composition	$t_{\text{high sal}}$ flood [h]	$t_{\text{low sal}}$ flood [h]	low sal effect	Avg $\Delta\phi_{\text{high sal}}$ last 24 h [$^{\circ}$ /h]	Avg $\Delta\phi_{\text{low sal}}$ [$^{\circ}$ /h]	ϕ at end of high sal [$^{\circ}$]	$t_{\text{detachment}}$ low sal [h]
1--14	[-]	[-]	[-]	[-]				
15	$\frac{1}{8}$ Morrow Brine	43,5	33	yes	$0,4 \pm 0,2$	$1,2 \pm 0,5$	60 ± 8	17 ± 11
16	Aborted	24	[-]	[-]				
17	$\frac{1}{8}$ Morrow Brine	112	101	yes	$0,1 \pm 0,2$	$0,5 \pm 0,2$	78 ± 10	49 ± 23
18	$\frac{1}{4}$ Morrow Brine	64,5	70,5	no				
19	Aborted	26	[-]	[-]				
20	$\frac{1}{4}$ Morrow Brine	73	67	yes	$0,12 \pm 0,09$	$0,7 \pm 0,3$	60 ± 9	20 ± 18
21	Aborted	113	[-]	[-]				
22	$\frac{1}{4}$ Morrow Brine	21,5	24	no				
23	$\frac{1}{4}$ Morrow Brine	21	70	no				
24*	$\frac{1}{8}$ Morrow Brine	[-]	46,5	no				
25	Aborted	48	[-]	[-]				
26	$\frac{1}{16}$ Morrow Brine	69,5	47	yes	$0,2 \pm 0,2$	$0,7 \pm 0,3$	66 ± 12	30 ± 14
27	$\frac{1}{4}$ Morrow Brine	48	100+	no				
28*	6,5 g/L NaCl	[-]	26	no				
29*	1,625 g/L NaCl	[0]	21	no				
30	$\frac{1}{16}$ Morrow Brine	29	65	no				
31	Aborted	46		[-]				
32	$\frac{1}{16}$ Morrow Brine	20	96	no				
33	Aborted	4		[-]				
34	$\frac{1}{16}$ Morrow Brine	46	114	yes				

During the first 14 experiments the new clay deposition method was tested and the protocols were established. In order to get the desired equilibrium, the experiments in this report sometimes took days to complete, just for high salinity flooding. After sometimes 2 - 4 days of high salinity flooding, another 1 – 2 days of low salinity flooding had to be recorded.

4.2 Determining the optimum clay patch size vs. clay concentration (for Montmorillonite)

In order to make the new experimental method that is described in section 3.1 work, an optimum clay patch concentration (and size), in relation to the placed oil volume, needed to be found first. For it turned out that if the amount of clay on the glass (i.e. the clay concentration in the clay suspension) was too low, the oil would not attach to the clay patch when flooded under water. On the other hand, when the amount of clay on the glass was too large, the oil droplets had a hard time to detach, even during low saline flooding. It is very well possible that the oil droplets would eventually also detach in a case of high clay concentration, but that in such a case it takes a longer time before the low salinity effect kicks in. But even if that were the case it still wouldn't be relevant to continue the experiments in this way. Because in order to perform as much experiments as possible, one must also choose the fastest way of executing them. And in a case of high clay concentration this is not the case.

But simply by knowing that oil immediately detaches when the clay amount is small, and that it hardly detaches when it is too large, one could say that there must be some clay amount in between those two extremes that is optimum, i.e. no immediate oil detachment or very strong oil attachment. It turned out that an ideal balance was found with a clay suspension that contained 160 mg/l, while the clay patch size was made with a droplet of approximately 6 μl .

To find the optimum concentration of the clay suspension and clay patch size, a series of different clay suspensions and clay patch sizes have been tested. The clay patch sizes were investigated by varying them from 2 μl up to 12 μl . These clay patches needed some amount of clay in it, but at this point it was still unknown which amount actually was suitable. So by systematic experimentation, the concentration about 160 mg/l was found. It turned out the oil, even in high salinity, detached relatively quick (within 0 up to 18 hours) when it was flooded on a 100 mg/l clay patch, while no significant contact angle change – let alone oil detachment – was observed on 250 mg/l clay patches after 96 hours. See also figure 4.1 and appendix 2.

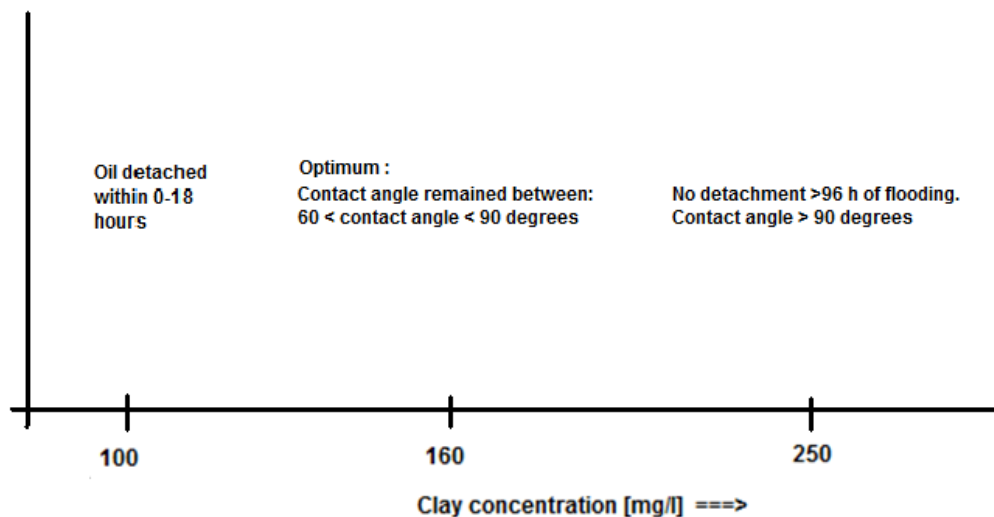


Figure 4.1: Detachment time of the oil drops as a function of clay concentration.

With help of the observations shown in Figure 4.1, the clay concentration was set to 160 mg/l so the oil would not attach too strongly but also not too weakly. When the required clay suspension was set to 160 mg/l, the clay patch sizes were varied from 2 μl to 12 μl in order to see what influence the size has on one oil attachment/detachment. See Figure 4.2a and 4.2b.

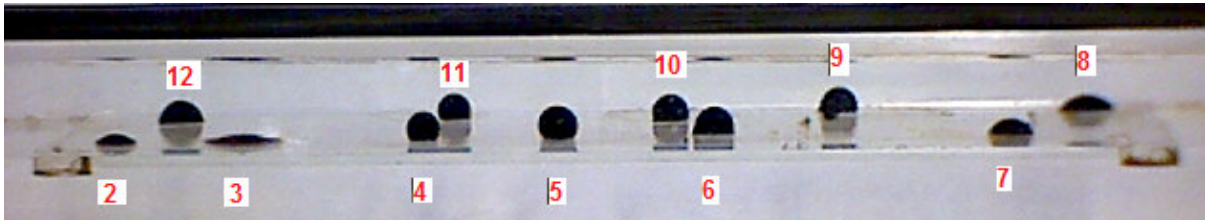


Figure 4.2a: In this experiment the clay patches, on which the oil is attached, are varied from 2 μl up to 12 μl . The oil volume was kept constant at 6 μl and the used water was high saline Morrow brine.

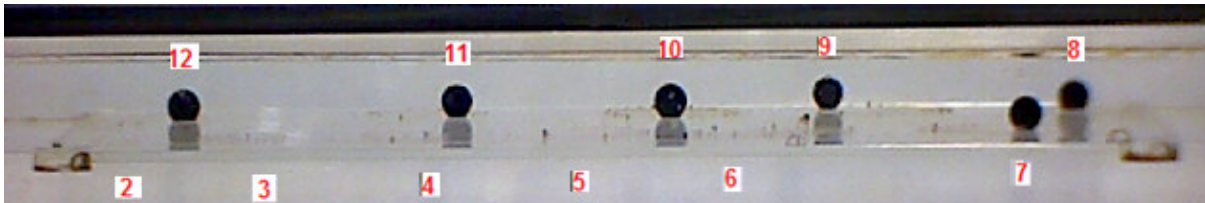


Figure 4.2b: End of high saline exposure (approximately 66 hours later). It is clear that only the oil drops on the 2,3,4,5 and 6 μl clay patches detached, and the rest did not.

From the images above it is clear that the oil droplets that are attached to the smaller clay patches, are more likely to detach. Although the oil droplets that were attached to the 7 μl to 12 μl clay patches did not detach, it is nevertheless clear the wetting changed to more water-wet because the contact angle decreased. For example, the oil-droplets in Figure 4.2b that are attached to the 9 μl and 11 μl clay patch don't bind the oil much, which indicates that the adhesion force that holds the oil to the clay has become weak.

4.1.1 Influence of clay patch shape

To explain this variety in attachment, while the conditions under which the oil droplets were flooded are the same, it seems to be important to also look at the way these clay patches are formed as a function of placed volume. Because when a certain volume from the clay suspension is taken and placed on the glass slide, the droplet will have a tendency to “spread” over the surface when its volume is too big. See Figure 4.3a and 4.3b. Both figures started with a volume of 2 μl up to 13 μl in Figure 4.3a and up to 12 μl in Figure 4.3b.

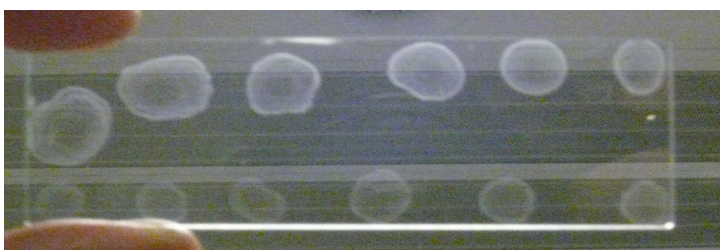


Figure 4.3a: Clay patches of 2 μl to 13 μl . Note how the clay patch area is proportional to the placed clay suspension volume.



Figure 4.3b: Clay patches of 2 μl to 12 μl . Note how the clay patch area is not proportional to the placed clay suspension volume. Especially the clay patch area of the 5 μl and 10 μl clay patch.

In Figure 4.3a the area of the clay patches are proportional to the placed clay suspension volume (from the lower left corner counter clock wise all the way up to 13 μl). But in Figure 4.3b this is not the case. It is clearly that the 5 μl and 10 μl clay patch are out of proportion considering the initial placed clay suspension, since the area of the 5 μl clay patch is bigger than the 6 and 7 μl clay patch. The same goes for the area of the 10 μl clay patch that is bigger than the area of the 11 and 12 μl clay patch.

As it was mentioned before, this variety in clay patch size is due to the “spreading” of the clay suspension volume when placed on the glass slide, with the effect that the amount of clay per unit of area decreases in comparison to the rest of the clay patches. This spreading has in turn to do with varieties in the glass surface, but most of all with placing the droplets by hand and not in an automated way. The droplet that comes out of the pipette, is always jiggling a bit due to the natural movement of the hand. And in some cases these droplets, when placed on the glass slide, absorb this “jiggling” motion of the hand which causes the droplet to break and spread over the surface.

Experience showed that this “spreading” of clay suspension happens significantly more often when its volume goes above 7 μl . Just to be sure that this spreading is avoided as much as possible, the clay patch size was from than one set to 6 μl , in spite the fact that the oil droplet that was placed on this clay patch had detached during high salinity flood, see Figure 4.2b. These conditions, the 6 μl clay patch size and 160 mg/l clay concentration, have been put to the test in a controlled environment which later on proved the low salinity effect. The results of this experiment will be discussed in the next paragraph.

4.3 Experimental approach

The first task in this project was to check whether previous results could be reproduced. One could say the low salinity effect is successfully reproduced when at least one of the following criteria is observed during the experiments:

- Detachment of the oil droplets when exposed to low salinity water, after extensive high saline flooding.
- Change of contact angle to a more water-wet state when exposed to low saline water, while during high saline exposure no visible change in contact angle has been observed for a relatively long period of time.

So in summary; a test was considered successful when little or no oil droplets detached during high salinity, hence the contact angle reached equilibrium, while during exposure to low salinity water this equilibration is disturbed by showing a decrease in contact angle and contact area.

4.4 Experimental results exhibiting the Low Salinity effect

In this section results using the new experimental methodology are shown that give new insights into the low salinity effect. Oil drops are allowed to equilibrate at high saline water and exposing them afterwards to low saline water. When the oil droplets show a clear change in contact angle (and/or change in contact area) when exposed to low saline water, this can be conceived as a positive low salinity effect. In figures 4.4 – 4.7 the contact angle (and contact area) change for a series of oil droplet is plotted as a function of time. Each plot shows a selection of droplets of one single experiment where between experiments the concentration of salt in the low saline water was varied. Also note that figures 4.4 – 4.7 show just a selection of the recorded data in order to improve the clarity of the figure. Therefore in the following figures only the droplets that showed the most significant sign of low salinity effect are presented here. To see the figures that show the contact angle change of all the droplets, see figures A3.1 – A3.4 in appendix 3.

The data shows experimentally how exposure to low salinity water causes the oil to decrease its adhesion to the clay, and ultimately even detachment.

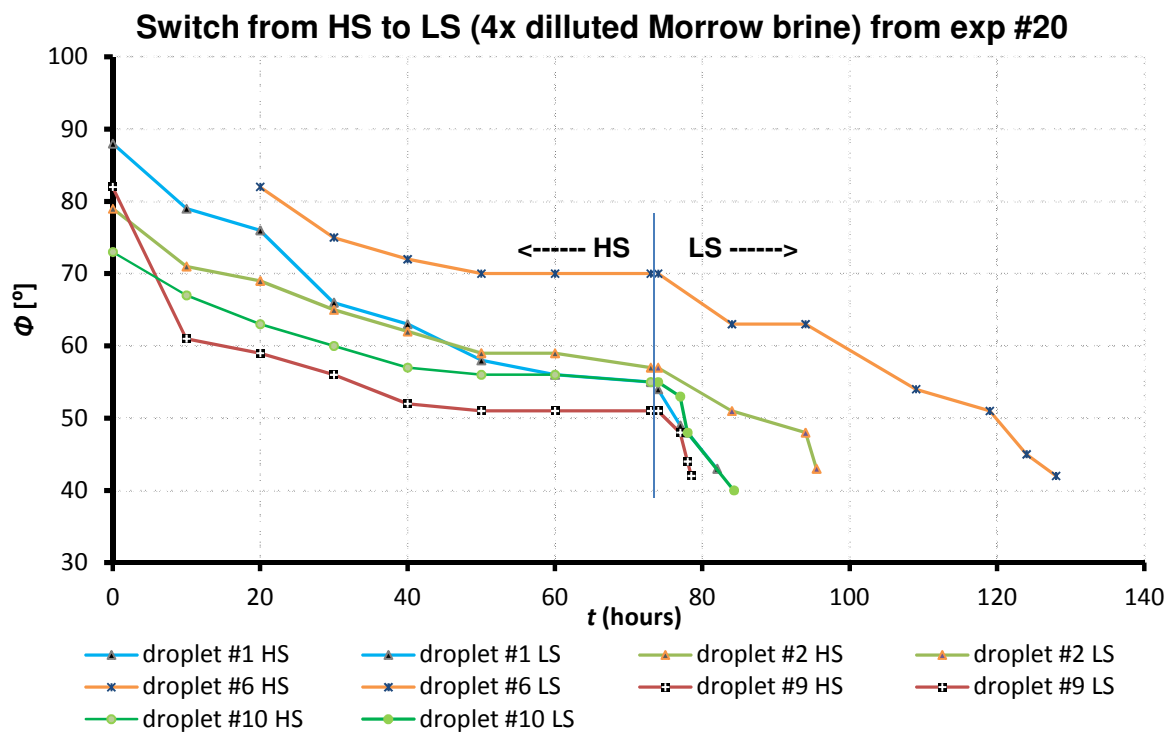


Figure 4.4a: Plotted contact angle change as a function of time. After 74 hours the equilibrated droplets were exposed to 4x diluted Morrow brine and soon afterward showed a significant change in contact angle and even detachment due to the lower salinity.

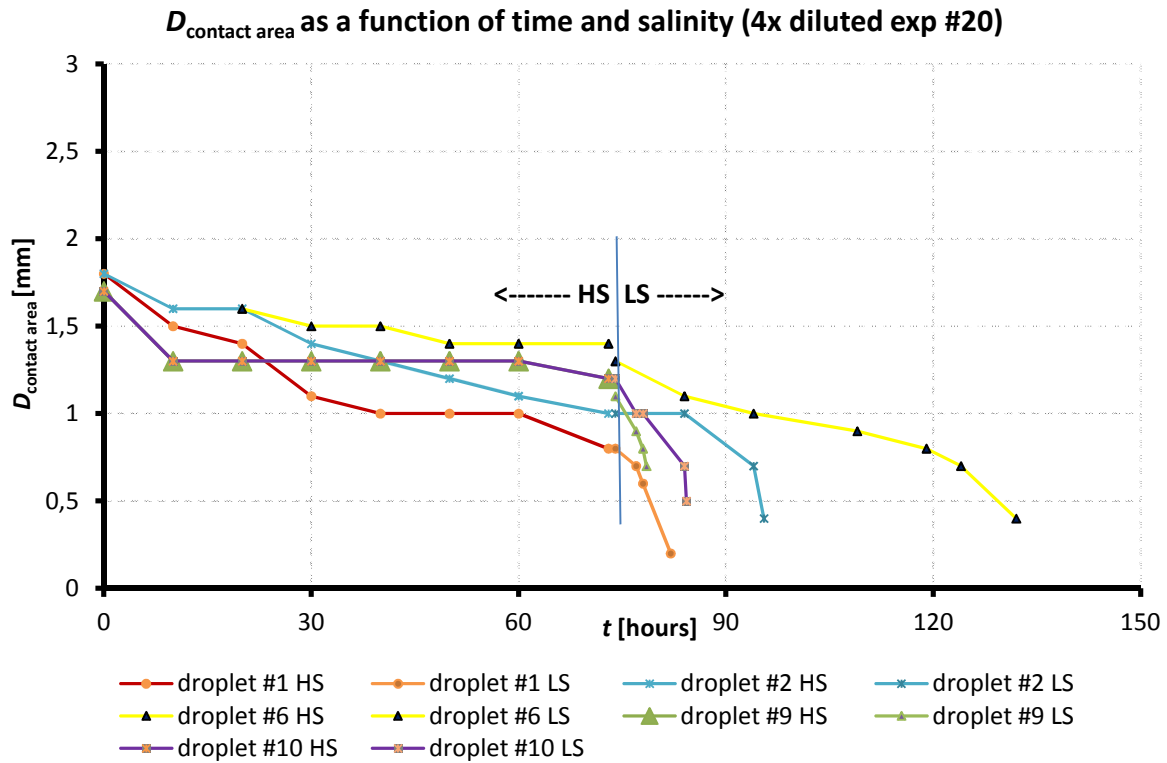


Figure 4.4b: The change in diameter of the contact area between oil and clay plotted as a function of time for experiment #20 when it was exposed to 4x diluted Morrow brine low saline water.

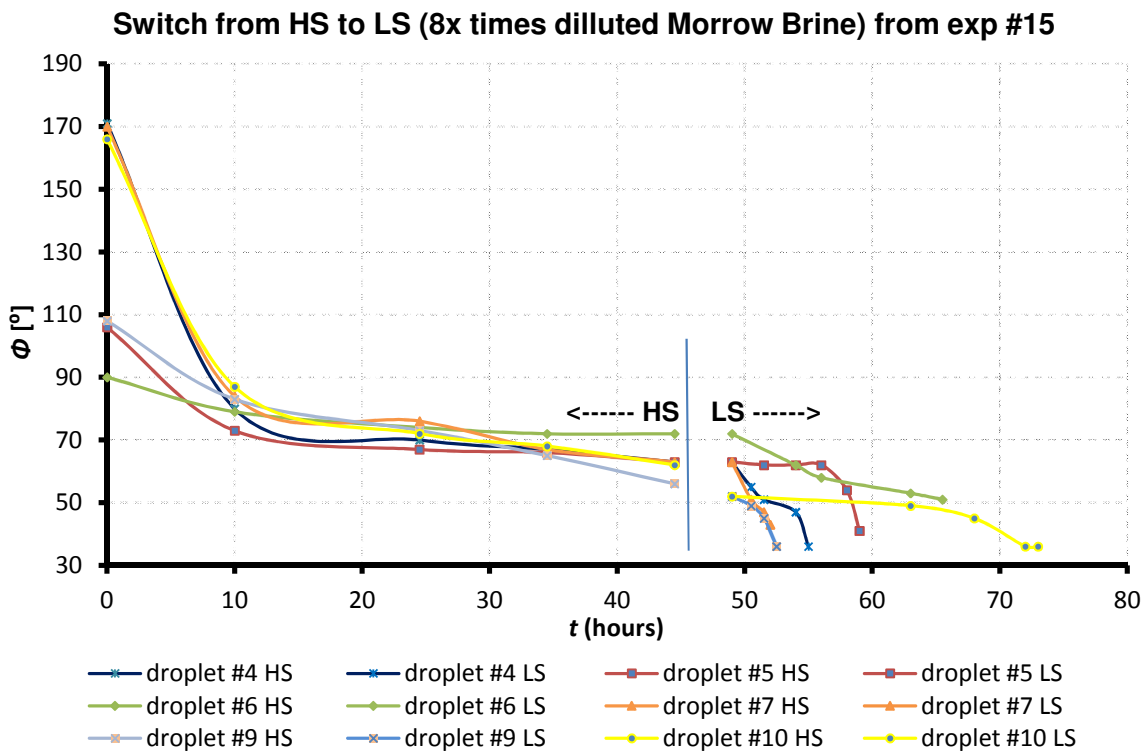


Figure 4.5a: Plotted contact angle change of oil droplets that showed a significant change in contact angle when it was exposed to 8x diluted Morrow brine low saline water. The low saline flooding started after 45 hours, but due to camera issues the recording started 4,5 hours later.

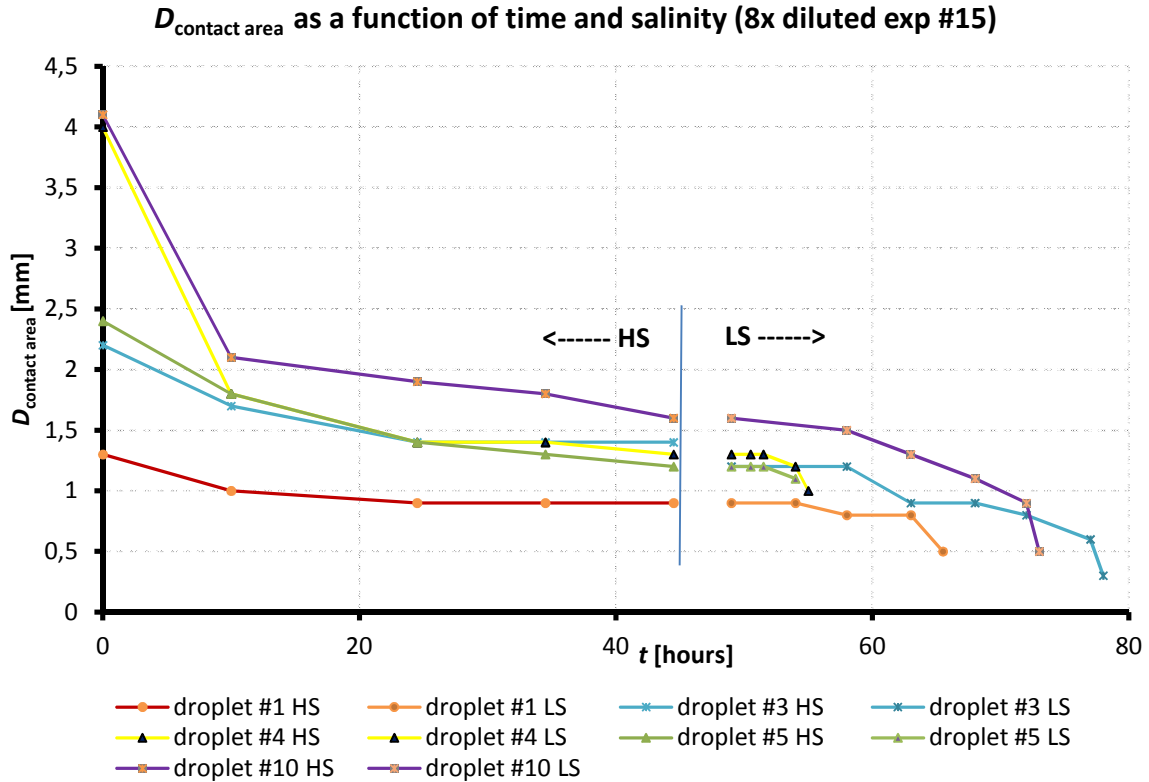


Figure 4.5b: The change in diameter of the contact area between oil and clay plotted as a function of time for experiment #15 when it was exposed to 8x diluted Morrow brine low saline water.

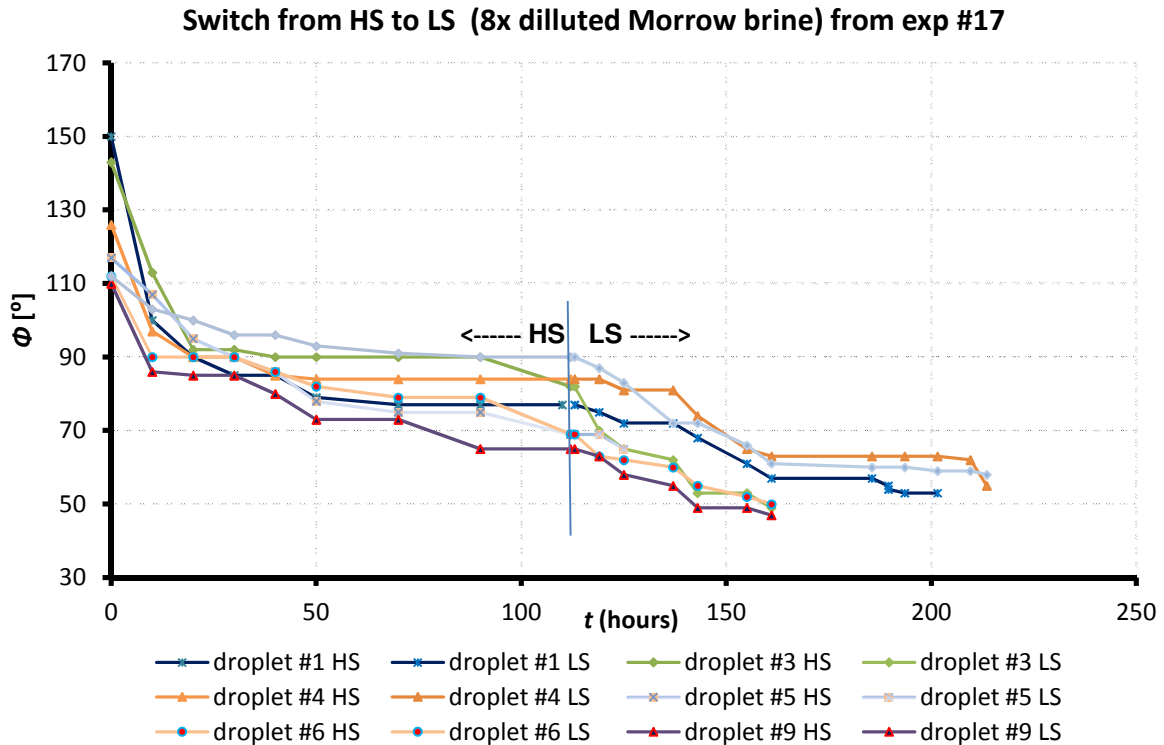


Figure 4.6a: The purpose of this experiment was to reproduce the same results from figure 4.4. But during this experiment the HS flooding was extended up to 112 hours so the droplets would have a longer time to equilibrate. Although droplet #1 and #4 did show a low salinity effect, it wasn't recorded that these droplets detached. This because a new experiment had de be set up. Furthermore, the exact detachment time of droplet #3, #6 and #7 is not known due to recording issues that night. It nevertheless is within the range of ± 6 hours.

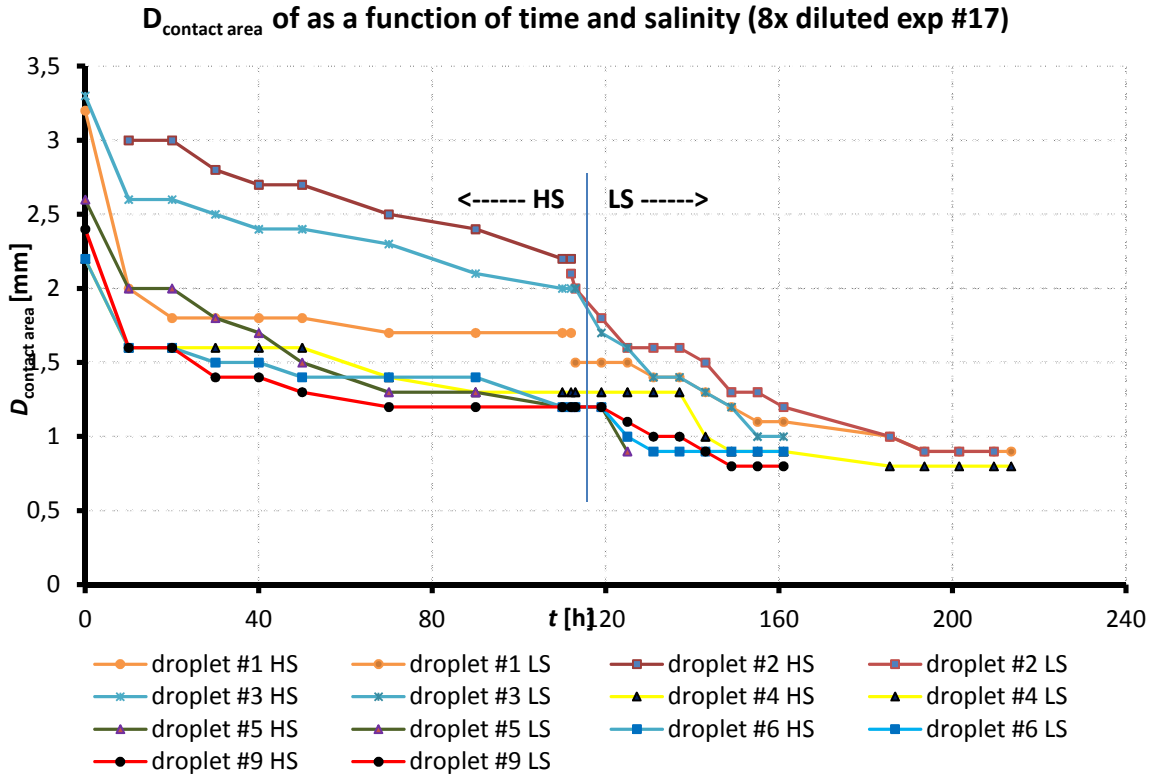


Figure 4.6b: The change in diameter of the contact area between oil and clay plotted as a function of time for experiment #17 when it was exposed to 8x diluted Morrow brine low saline water.

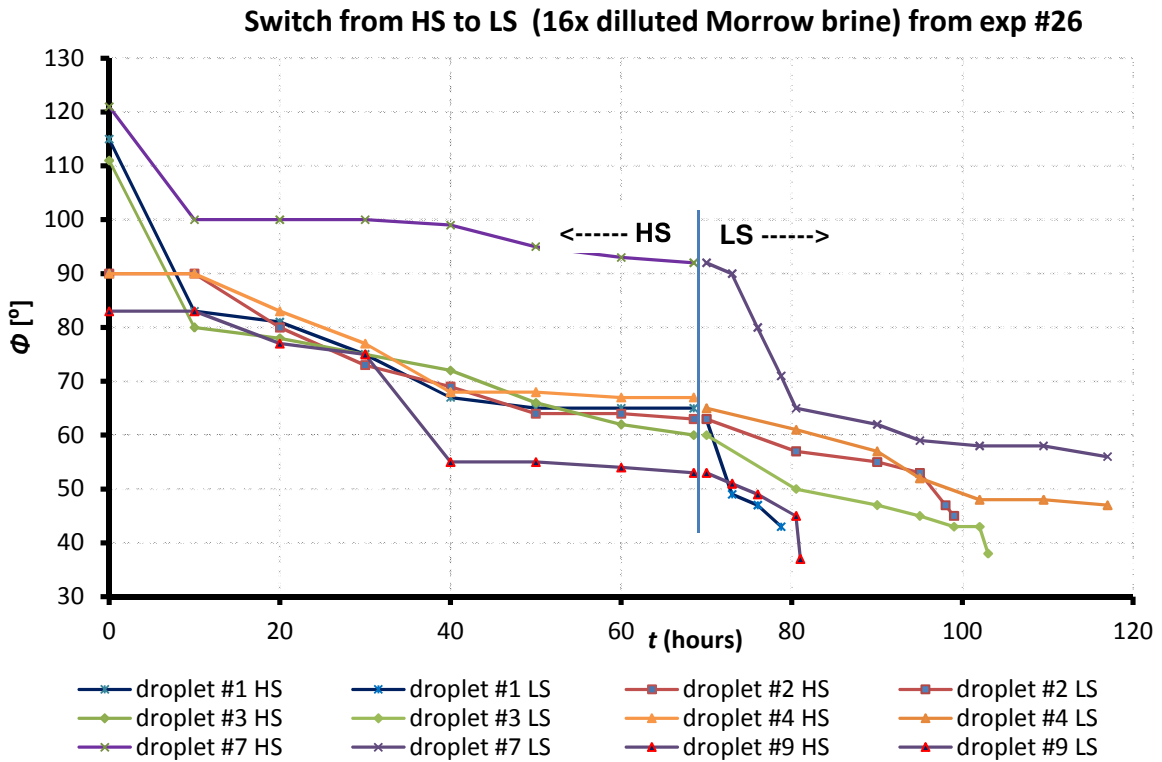


Figure 4.7a: Again the contact angle change is plotted as a function of time. But in this case the salinity for the low saline flooding is diluted 16 x in order to see if the detachment time of the oil droplets depends on the salinity. Also in this experiment droplets #4 and #7 have not detached to the end so that a new experiment could equilibrate during the weekend.

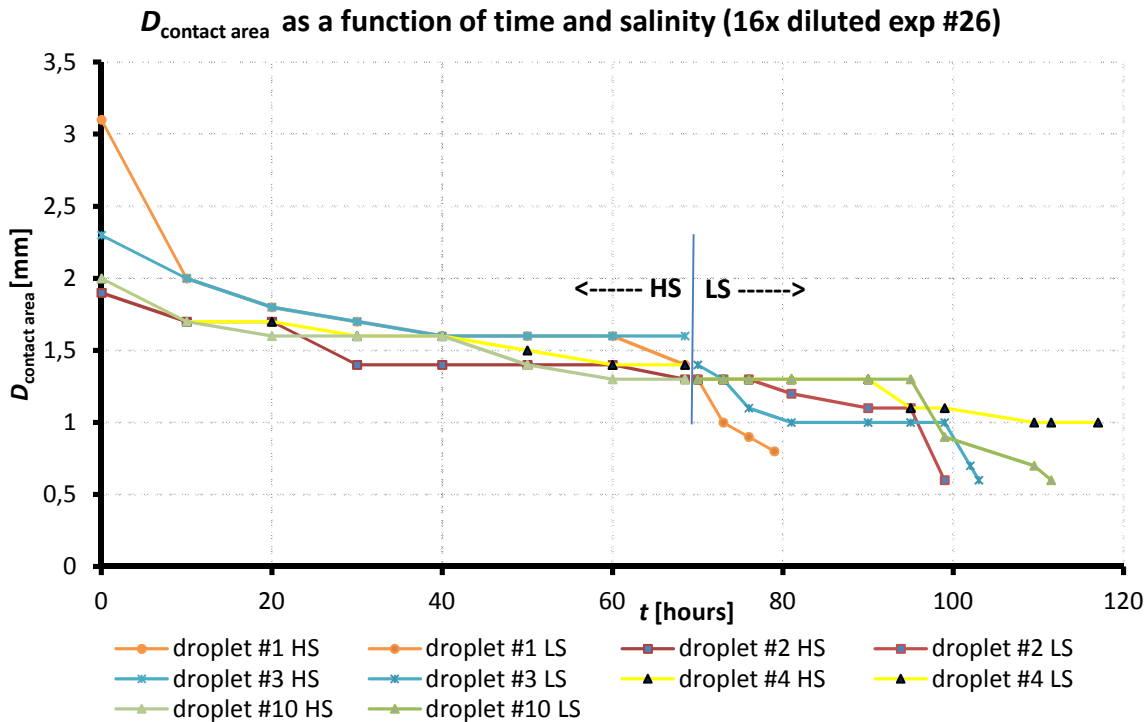


Figure 4.7b: The change in diameter of the contact area between oil and clay plotted as a function of time for experiment #26 when it was exposed to 16x diluted Morrow brine low saline water.

The oil droplets presented show a significant change in contact angle when they become exposed to low saline water, even when the uncertainty of 5 degrees is taken into account.

In the data some general trends can be observed:

1. When the initial contact area between the oil and clays, $A_{\text{contact area}}$, is high, then the detachment time of oil is long.
2. When the initial contact angle (at start of LS), $\phi_{\text{initial LS}}$, is relatively high, then the detachment time, $t_{\text{detachment}}$, is also relatively long.
3. When the volume of the oil that is attached to clay is high, then the detachment time is shorter.
4. Upon exposure to low salinity brine the contact angle typically decreases until a critical contact angle $\phi_{\text{crit}} \sim 40\text{-}45$ degrees is reached at which the droplet detaches.

All these observed trends to a large degree correct, when the detachment time is compared to the other droplets within the same experiment, see Tables 4.2, 4.3, 4.4 and 4.5. The data in the tables is sorted according to the detachment time of the droplets and not by droplet number. And note in case there is asterisk (symbol: *) next to the droplet number, that means that the measured diameter of the contact area has a higher uncertainty than initially stated at top of the table because in that particular case optimum measurement was not possible due to artifacts in the data.

Table 4.2: Detachment time of 4 dilution LS flooding as a function of initial contact angle, initial contact area and oil volume (exp #20).

droplet #	$t_{\text{detachment}}$ [h]	$\Phi_{\text{initial}} [^\circ] \pm 5^\circ$	$D_{\text{contact area}}$ [mm] $\pm 0,1$ mm	$A_{\text{contact area}}$ [mm ²]	$V_{\text{oil droplet}}$ [mm ³]
9	4,5	51	1,1	$1,0 \pm 0,2$	$3,3 \pm 0,7$
1	8,0	54	0,8	$0,5 \pm 0,1$	$2,8 \pm 0,6$
10	10,3	55	1,2	$1,1 \pm 0,2$	$3,1 \pm 0,7$
2	21,5	57	1,0	$0,8 \pm 0,2$	$3,3 \pm 0,7$
6	54	70	1,3	$1,3 \pm 0,2$	$3,8 \pm 0,8$

Table 4.3: Detachment time of 8x dilution LS flooding as a function of initial contact angle, initial contact area and oil volume (exp #15).

droplet #	$t_{\text{detachment}}$ [h]	$\Phi_{\text{initial}} [^\circ] \pm 5^\circ$	$D_{\text{contact area}}$ [mm] $\pm 0,1$ mm	$A_{\text{contact area}}$ [mm ²]	$V_{\text{oil droplet}}$ [mm ³]
7*	3,0	63	$1,0 \pm 0,2$	$0,8 \pm 0,2$	3 ± 1
9*	3,5	52	$1,1 \pm 0,2$	$1,0 \pm 0,2$	5 ± 2
4	6,0	63	1,3	$1,3 \pm 0,2$	5 ± 1
11*	8,0	68	$1,0 \pm 0,2$	$0,8 \pm 0,2$	6 ± 2
5	10,0	63	1,2	$1,1 \pm 0,2$	$2,2 \pm 0,6$
6*	16,5	72	$0,9 \pm 0,2$	$0,6 \pm 0,2$	$1,2 \pm 0,4$
1	16,5	49	0,9	$0,6 \pm 0,2$	$3,0 \pm 0,7$
10	24	61	1,6	$2,0 \pm 0,3$	6 ± 1
3	29	52	1,2	$1,1 \pm 0,2$	$3,8 \pm 0,8$

Table 4.4: Detachment time of 8x dilution LS flooding as a function of initial contact angle, initial contact area and oil volume (exp #17).

droplet #	$t_{\text{detachment}}$ [h]	$\Phi_{\text{initial}} [^\circ] \pm 5^\circ$	$D_{\text{contact area}}$ [mm] $\pm 0,1$ mm	$A_{\text{contact area}}$ [mm ²]	$V_{\text{oil droplet}}$ [mm ³]
5*	12	69	$1,2 \pm 0,2$	$1,1 \pm 0,4$	$2,1 \pm 0,7$
8*	33,5	64	$1,0 \pm 0,2$	$0,8 \pm 0,3$	$1,8 \pm 0,6$
3	66 ± 6	82	2,0	$3,1 \pm 0,3$	5 ± 2
6*	66 ± 6	69	$1,2 \pm 0,2$	$1,1 \pm 0,4$	$2,1 \pm 0,7$
9	66 ± 6	65	1,2	$1,1 \pm 0,2$	$2,2 \pm 0,6$
10	101+	90	2,1	$3,5 \pm 0,4$	5 ± 2
7*	101+	82	$1,7 \pm 0,2$	$2,3 \pm 0,6$	$2,9 \pm 0,9$
4	101+	84	1,3	$1,3 \pm 0,2$	$1,4 \pm 0,5$
1	101+	77	1,5	$1,8 \pm 0,3$	$2,9 \pm 0,8$
2	101+	93	2,1	$3,5 \pm 0,4$	6 ± 2

Table 4.5: Detachment time of 16x dilution LS flooding as a function of initial contact angle, initial contact area and oil volume (exp #26).

droplet #	$t_{\text{detachment}}$ [h]	$\Phi_{\text{initial}} [^\circ] \pm 5^\circ$	$D_{\text{contact area}}$ [mm] $\pm 0,1$ mm	$A_{\text{contact area}}$ [mm ²]	$V_{\text{oil droplet}}$ [mm ³]
1	8,75	63	1,3	$1,3 \pm 0,2$	6 ± 1
9*	11	53	$1,1 \pm 0,2$	$1,0 \pm 0,4$	$2,6 \pm 0,8$
2	29	63	1,3	$1,3 \pm 0,2$	$3,2 \pm 0,7$
3	33	60	1,4	$1,5 \pm 0,3$	$3,7 \pm 0,8$
10	41,5	60	1,3	$1,3 \pm 0,2$	$3,7 \pm 0,8$
4	47+	65	1,3	$1,3 \pm 0,2$	$3,1 \pm 0,8$
7*	47+	92	$1,8 \pm 0,2$	$2,5 \pm 0,6$	3 ± 1

To show that the stated trends are valid, the data presented in Tables 4.2 – 4.5 will be briefly reviewed. For instance in Table 4.2 one can see droplet #9 detached after approximately 4,5 hours during low saline flooding, whereas droplet #6 detached after 54 hours. This relatively large difference in detachment time is easily explained when the values of the initial contact angle, initial contact area (or initial contact diameter) and the attached oil volumes are compared. Droplet #6 has an initial contact angle of 70°, while the initial contact angle of droplet #9 is only 51°. This means that droplet #6 adheres much stronger to the clay than droplet #9, see equation 2.6. Also the initial contact area (or contact diameter) is larger in droplet #6, which is also a sign of stronger bonding between the oil and clay. The same could also be argued for the remaining droplets showed in Table 4.2. However, a few examples can be found in which the describes trends do not hold. For example droplets #5 and #8 from Table 4.4, and droplets #5 and #6 of Table 4.5. A reason for this deviation could not be found.

Difficulties are encountered when attempting to derive specific correlations from these general trends because – caused by the experimental approach - the droplets have very different equilibration angles, contact areas, volume sizes and therefore also very different detachment times. In section 4.5 and 4.6 an attempt is made to normalize these differences. For instance, it could be possible that the detachment time is a function of the salinity, initial contact area, initial contact angle, oil volume or even the presence of divalent cations. In Figure 4.4 (4x diluted MB) and Figure 4.5 (8x diluted MB), whenever there is a change in contact angle, this is always accompanied by a change in diameter of the contact area. But for the figures 4.6 (8x diluted) and 4.7 (16x diluted), this is not the case. The reason why the change in contact angle in Figures 4.6 and 4.7 is not always accompanied by a change in contact area, is due to the large initial contact diameter of the droplets in these experiments. The average diameter of the contact area in Figures 4.4b and 4.5b is approximately 1 mm. Whereas the average diameter of figures 4.6.b and 4.7b is approximately 1,5 mm. That's why it is argued that this detachment of oil is the result of some diffusion mechanism, see section 4.5.

In the following, the variation in detachment time is systematically taken into account by making use of the first observed trend, which stated that droplets with large contact area $A_{\text{contact area}}$, require long detachment times. That could actually be an indication that equilibration from high saline to low saline brine in the clay layer under the oil droplet is transport limited, for instance by a diffusion process. That will be discussed in the following section.

4.5 Is the process controlled by diffusion?

In this section experimental evidence is provided that a diffusion mechanism is involved in the kinetics of oil detachment by showing that the detachment time of oil droplets is on the same order of magnitude as a diffusion time.

The observation that larger contact areas lead to longer detachment times could mean that there is a diffusion process of salt ions involved. The basic idea is that initially the salt concentration is high, i.e. high salt concentration around the oil droplet but also in the clay layer between oil droplet and glass substrate. The amount of time it takes for the low saline concentration ‘penetrates’ and replaces the high saline water film under the oil can be seen as a diffusion time and is given by equation 4.1 [21]. Also see Figure 4.8 for an illustration of this diffusion process.

$$t_{\text{diffusion}} = \frac{r^2}{4 \cdot D} \quad 4.1$$

Where: r is the radius of the contact area between oil and clay at start of LS flood [mm]

D is the diffusion constant for salt water was estimated at 10^{-9} [mm²/s]

$t_{\text{diffusion}}$ is the diffusion time [s]

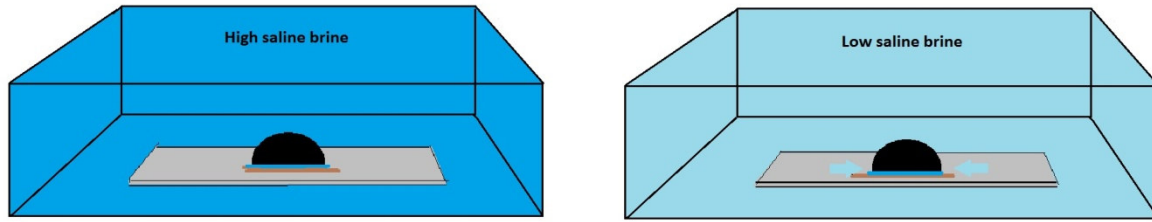


Figure 4.8: Illustration of the diffusing water film underneath the droplet.

When the salinity is lowered, the concentration of salt in the surrounding will immediately change because of convective exchange, but the salt concentration in the clay layer is not accessible to convection and therefore only exchange by diffusion is possible, see Figure 4.8. In order to check whether a diffusion mechanism is compatible with the experimental data, a linear diffusion model is used to estimate the time it would take until the salt concentration under the oil droplet has decreased from the initial concentration c_0 to a fraction $1/a$.

In a linear diffusion equation the time evolution of the concentration profile $c(r,t)$ is given by:

$$c(r,t) = c_0 \operatorname{Erfc}\left(\frac{r}{\sqrt{4Dt}}\right) = \frac{c_0}{a} \quad 4.2$$

Where Erfc is the complementary error function. For the concentration the centre ($r=0$) having reached a value c_0/a this equation

$$c(r,t) = c_0 \operatorname{Erfc}\left(\frac{r}{\sqrt{4Dt}}\right) = \frac{c_0}{a}$$

is numerically solved using Mathematica. In Table 4.6 the solutions are listed for a set of values of a showing how the time to decay an initial concentration to $1/a$ increases with a .

Table 4.6: Showing the different diffusion times at different fraction of a

a	$y = \frac{r}{\sqrt{4Dt}}$	$t_{\text{dif}} = \frac{r^2}{4Dy^2}$; $r = 2\text{mm}$, $D = 10^{-9} \text{ m}^2/\text{s}$
1.15	1	0.28 h
2	0.477	1.22 h
5	0.12	19.3 h
10	0.09	34 h

For typical low salinity water flooding operations, 5000 TDS is used as low salinity, i.e. from the Morrow brine with approximately 26000 TDS, the decrease is $1/5$ meaning that $a=5$. That is also compatible with the previous observations [15]. See Figure 4.9.

Therefore a typical diffusion time for an oil droplet with a 2 mm radius is 20 h, which is also the time scale of typical detachment times in the experiment, see Tables 4.7 – 4.10

Now, the diffusion constant from equation 4.1 and 4.1 is estimated roughly by equation 4.3 [23].

$$D = \frac{R \cdot T \cdot [(1/z_+) + (1/z_-)]}{F^2 [(1/\lambda^0_+) + (1/\lambda^0_-)]}$$

4.3

Where: D is the diffusion constant at low salt concentrations [cm^2/s]

R is the gas constant, $8,314 \text{ J}/(\text{mol}\cdot\text{K})$

T is the absolute temperature [K]

λ^0_+, λ^0_- is the limiting ionic conductances of the cation and anion, see appendix 4 [A/cm^2]

z_+, z_- is the valence of the cation and anion, respectively [-]

F is the Faraday constant $95.600 \text{ C}/\text{mol}$

Magnesium has a valence of 2 and limiting ionic conductance of $53,1 \text{ A}/\text{cm}^2$. Chlorine on the other hand has a valence of 1 and limiting ionic conductance of $76,3 \text{ A}/\text{cm}^2$. Filling this in equation 4.1 gives:

$$D_{\text{MgCl}_2} = \frac{8,314 \cdot 293 \cdot [(1/2) + (1/1)]}{95.600^2 [(1/53,1) + (1/76,3)]} = 1,25 \cdot 10^{-5} \text{ cm}^2/\text{s} = 1,25 \cdot 10^{-7} \text{ mm}^2/\text{s}$$

The same calculation could be made for the remaining salts, of which the results are presented below.

D_{NaCl} is: $1,61 \cdot 10^{-7} \text{ mm}^2/\text{s}$, D_{CaCl_2} is: $1,33 \cdot 10^{-7} \text{ mm}^2/\text{s}$, D_{KCl} is: $2,00 \cdot 10^{-7} \text{ mm}^2/\text{s}$. Averaging these four different diffusion constants results in $(1,5 \pm 0,5) \cdot 10^{-7} \text{ mm}^2/\text{s}$.

Table 4.7: Diffusion time of the droplets in 4x diluted MB (exp #20)

droplet #	$(r_{\text{contact area}} \pm 0,05) [\text{mm}]$	$t_{\text{detachment}} [\text{h}]$	$t_{\text{diffusion}} [\text{h}]$
9	0,55	4,5	0,8
1	0,40	8,0	0,5
10	0,60	10,3	1,2
2	0,50	21,5	0,8
6	0,65	54	1,2

Table 4.8: Diffusion time of the droplets in 8x diluted MB (exp #15)

droplet #	$(r_{\text{contact area}} \pm 0,05) [\text{mm}]$	$t_{\text{detachment}} [\text{h}]$	$t_{\text{diffusion}} [\text{h}]$
7*	$0,5 \pm 0,1$	3,0	1
9*	$0,5 \pm 0,1$	3,5	1
4	0,65	6,0	1,2
11*	$0,5 \pm 0,1$	8,0	1
5	0,60	10,0	0,8
6*	$0,5 \pm 0,1$	16,5	0,7
1	0,45	16,5	0,7
10	0,80	24	2
3	0,60	29	1,2

Table 4.9: Diffusion time of the droplets in 8x diluted MB (exp #17)

droplet #	$(r_{\text{contact area}} \pm 0,05)$ [mm]	$t_{\text{detachment}}$ [h]	$t_{\text{diffusion}}$ [h]
5*	0,6 ± 01	12	1,2
8*	0,5 ± 0,1	33,5	0,8
3	1	66 ± 6	3
6*	0,6 ± 0,1	66 ± 6	1,2
9	0,6	66 ± 6	0,7
10	1,05	101+	3
7*	1,35	101+	1,8
4	0,65	101+	1,2
1	0,75	101+	1,8
2	1,05	101+	4

Table 4.10: Diffusion time of the droplets in 16x diluted MB (exp #26)

droplet #	$(r_{\text{contact area}} \pm 0,05)$ [mm]	$t_{\text{detachment}}$ [h]	$t_{\text{diffusion}}$ [h]
1	0,65	8,75	1,2
9*	0,55 ± 0,1	11	1
2	0,65	29	1
3	0,70	33	1,4
10	0,65	41,5	1,4
4	0,65	47+	1,4
7*	0,9 ± 0,1	47+	2,6

Tables 4.7 – 4.10 display that diffusion times order of several hours are in a similar range as experimentally observed detachment times. Note that the estimated diffusion times depend on the fraction $1/a$ that an initial concentration has decreased to until a droplet detaches. This fraction is not exactly known and only a rough estimate like the linear diffusion model. Those approximations can introduce easily a factor of 10 longer diffusion times. In other words, within its own range of uncertainty, diffusion is a plausible mechanism influencing the detachment kinetics.

In order to refine this model, more research is required. Modeling of the diffusion processes could in reality be much more complicated than approximated by equation 4.1 and 4.2 because it is not a linear but a radial problem including a gradual process with a “peeling off” detachment of the oil.

4.5.1 Dimensionless parameters

Now that the diffusion time is calculated, a new parameter can be introduced that normalizes the data for the fact that all the droplets, from every experiment, have a different contact area. This parameter is defined by dividing the actual detachment time by the calculated diffusion time, see equation 4.3.

$$t_{\text{dim.less}} = \frac{t}{t_{\text{diffusion}}} = \frac{y^2 \cdot 4 \cdot D \cdot t}{r^2} \quad 4.3$$

Where: $t_{\text{dim.less}}$ is the dimensionless time [-]

$t_{\text{diffusion}}$ is the diffusion time for the particular droplet [h]

t is actual detachment of the droplet since the start of low salinity flood [h]

r is the radius of the contact area between oil and clay at start of LS flood [mm]

D is the diffusion constant, $(1,5 \pm 0,5) \cdot 10^{-4}$ mm²/s

In the previous study of this project, a plot is made in which oil production is plotted as a function of Total Dissolved Solids (TDS), see figure 4.9. (See table 3.2 for more information about the meaning of TDS). Figure 4.9 shows that oil production depends on whether the clay shows signs of formation damage.

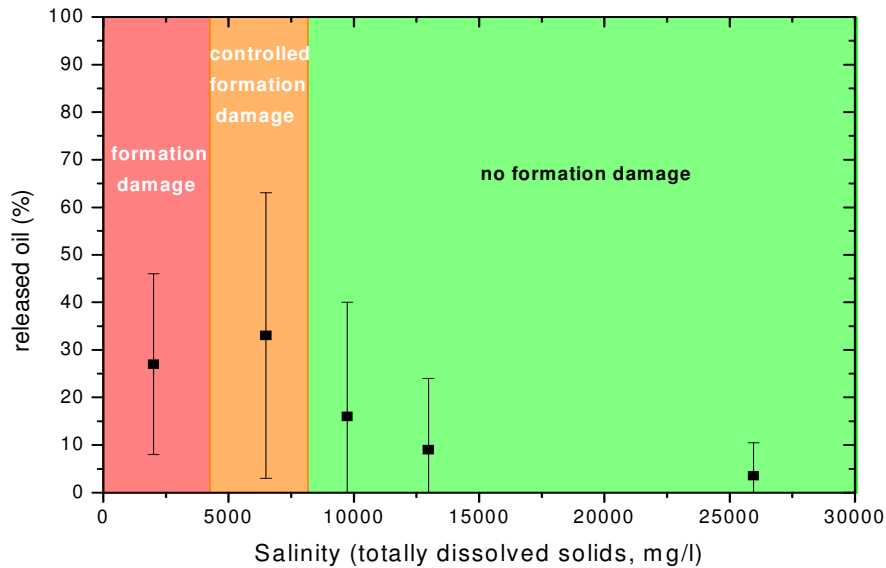


Figure 4.9: Amount of released (detached) oil as a function of the brine salinity (in totally dissolved solids, mg/l) on Montmorillonite clay patches [15].

The amount of clay that was used for the experiments in this study was significantly less than in the previous study, so actual formation damage in the form of clay swelling could not be observed. But nevertheless, assuming that the clays in this study swell on the same salinities, and therefore show sign of formation damage on the same salinities, similar clay swelling regimes would apply and a similar plot as in Figure 4.9 can be made for the data in this study. Instead of the release oil, the dimensionless time is plotted.

See figure 4.10. In this Figure the dimensionless time is averaged for all the droplets that responded to the low salinity water, and then plotted as a function of salinity.

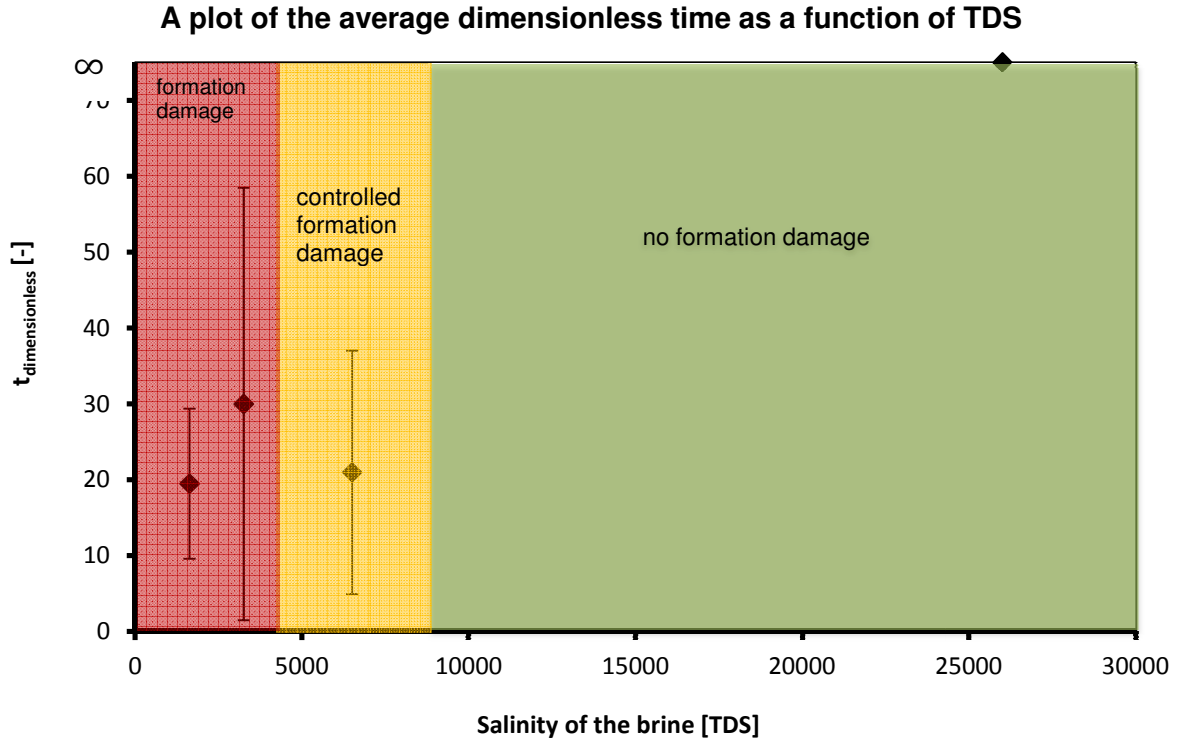


Figure 4.10: Averaged dimensionless time of oil droplets on Montmorillonite clays, plotted as a function of brine salinity. Note that the dimensionless time for the undiluted brine is towards infinity, because it is unlikely it would detach.

In Figure 4.10, the dimensionless time for the undiluted brine is set to infinity, because the dimensionless time is defined as the detachment time divided by the diffusion time, see equation 4.3. With this in mind, one could argue that therefore a high dimensionless time represents a slower detachment of the oil. This slower detachment time of oil, hence dimensionless time, is in turn analogical to the oil production from Figure 4.9. In these regimes, however, no strong correlation in the data could be observed. The main reason is the relatively large variation in the data, limited optical resolution for the contact angle measurement and the relatively small number of successful experiments.

4.3.2 Additional normalization attempts

Furthermore, there are still two remaining factors that are not included in Figure 4.8. Namely, the initial contact angle and the volume of the oil. To include these factors also in the normalization, an extra factor to the dimensionless time has been included. This factor is defined by multiplying the dimensionless time with the difference in initial contact angle and the critical contact angle, ($\Phi_{\text{initial}} - \Phi_{\text{critical}}$). The value that is used for the critical contact angle is averaged for all the droplets and set to 42° .

The factor that normalizes the data for the fact that all the droplets have different oil volumes, is defined as the radius of the contact area to the power of two, divided by the radius of the oil droplet to the power of three, see equation 4.4.

$$\tau = t_{\text{dim.less}} \cdot (\phi_{\text{initial}} - \phi_{\text{critical}}) \cdot \frac{r_{\text{contact area}}^2}{r_{\text{droplet}}^3} \quad 4.4$$

Where: τ is the normalized parameter [$^{\circ}/\text{mm}$]

Φ_{initial} is the contact angle at start of low salinity flooding [$^{\circ}$]

Φ_{critical} is the critical contact angle, approximately 42°

This equation is derived from the trends explained in 4.2 and with the help of Excel. A large variation of possible correlations have been tested to see if there is an equation that collapses the data as much as possible and so decrease the spreading. This is done by calculating the standard deviation of τ within every experiment and dividing this by the average of τ . If the ratio of the standard deviation and average decreases when a change is made in equation 4.4, than this could be an indication that the data is showing possible trends. Unfortunately, this did not improve the normalization of the data significantly. But nevertheless, the average of the normalized parameter τ from equation 4.4 is plotted in Figure 4.11 as a function of TDS.

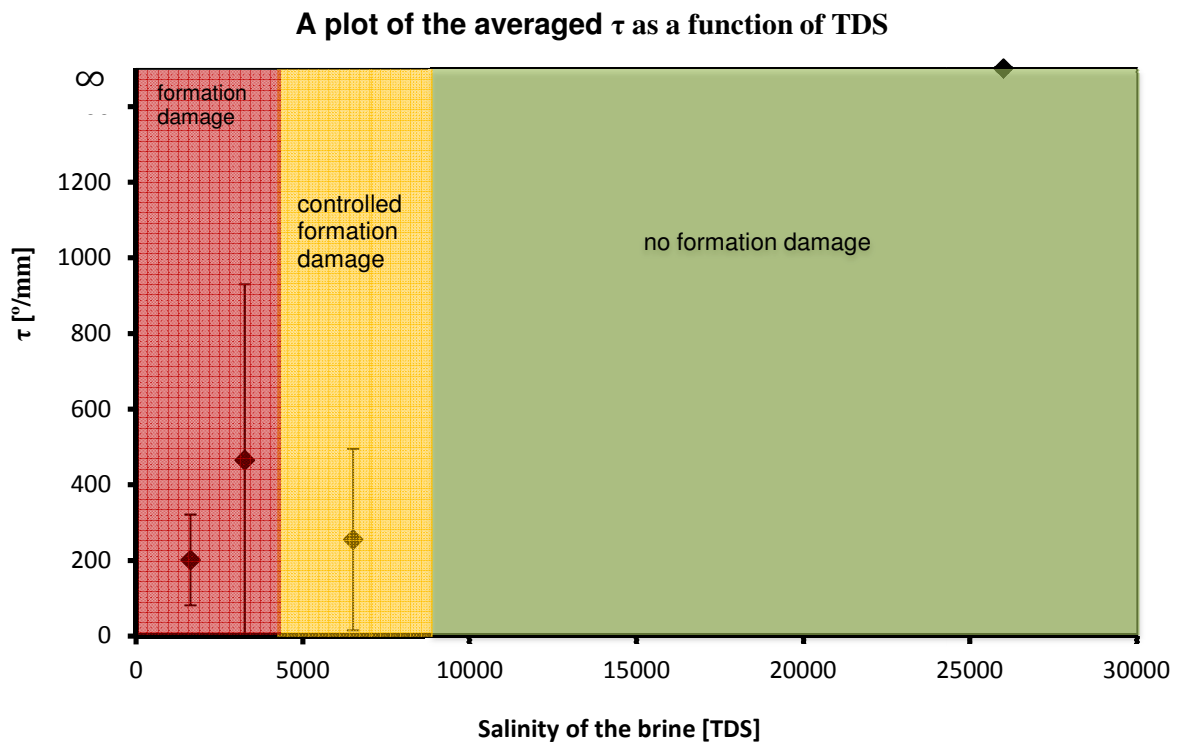


Figure 4.11: Averaged τ of the oil drops on Montmorillonite clays, plotted as a function of brine salinity.

5. Conclusions

The main aim of this work was to find additional insights in the low salinity effect with the new experimental methodology.

The first important conclusion that can be drawn is that without the presence of clay, oil does not permanently stick to glass substrates but detaches within few minutes. With the presence of clay, oil can form stable droplets over days. That means that clay make the otherwise strongly water-wet glass substrate actually oil-wet.

In the systematic study on the optimum clay concentration it was found that the amount of clay in the suspension was a crucial factor whether the oil drops would respond to the low salinity. If the amount of clay in the suspension was too high (>250 mg/l for Montmorillonite and >1100 mg/l for Kaolinite), than the oil drops adhered to strongly to the clays and ultimately no sign of the low salinity effect would be observed. However, when the amount of clay in the suspension was too low (<100 mg/l for Montmorillonite and <700 mg/l for Kaolinite), than the droplets would detach during the high salinity so the experiment had to be aborted. At the optimum concentration there was an approximate balance between buoyancy forces and adhesion forces, i.e. the optimum clay concentration is specific to the droplet size which in a reservoir rock would be much smaller than in this experiment. In other words, the clay concentration on a solid to bind oil can be much smaller.

With the new experimental methodology, parameters of the oil droplet such as contact angle and contact area were monitored over time and give further insight into the detachment kinetics of oil droplets upon exposure to low salinity brine. The first important finding was that upon exposure to low salinity brine the contact angle typically decreases until a critical contact angle $\Phi_{crit} \sim 40-45$ degrees is reached at which the droplet detaches. Caused by the experimental protocol, oil droplets varied in size (volume), initial contact area and initial contact angle. This variation gave additional experimental variables from the following observed general trends:

- (4) Droplets with larger volumes require less time to detach. That is indicative for the force balance acting on the contact area of the droplet: larger droplet volumes means larger buoyancy forces responsible for the detachment, i.e. larger buoyancy forces means shorter time to detachment.
- (5) An initially high contact angle (at start of LS), $\Phi_{initial\ LS}$, indicates stronger adhesion and as a consequence the detachment time, $t_{detachment}$, is also relatively long.
- (6) When the initial contact area between the oil and clays, $A_{contact\ area}$, is high, then the detachment time of oil is long.

The third trend can be interpreted as a diffusion controlled equilibration of salt ions in the clay layer between oil and glass substrate which critically influences the detachment kinetics of oil. The diffusion time scales were of the same order of magnitude as the experimentally observed detachment times. That supports the view that diffusion plays an important role in the detachment kinetics of oil. That finding might change the view how quickly a low salinity response in a core flooding experiment can be expected (apart from mixing between high and low salinity brine when injecting at a constant rate).

The detachment time was then normalized by the diffusion time in order to account for contact area variations. While in the high salinity regime stable droplets were found (meaning that detachment time is infinite), in the formation damage and controlled formation damage regime dimensionless detachment times 5-40 were found. Ideally in a diffusion controlled regime dimensionless times around 1 would be expected. The fact that a much wider range is observed reflects mainly the uncertainty in the estimate of the diffusion time, starting with approximating the diffusion coefficient, the linear diffusion model and the fraction of the initial salt concentration required for droplet

detachment. Nevertheless, within its own range of uncertainty the diffusion time scale is compatible with the data and therefore a plausible factor influencing the detachment kinetics.

Using the diffusion time as a normalization for the detachment times, in formation damage and controlled formation damage regimes, which indicate minor to large clay swelling, however, no strong correlation in the data could be observed. From an experimental side limiting factors are the relatively large variation in the data, limited optical resolution for the contact angle measurement and the relatively small number of successful experiments. It might as well be that in the formation and controlled formation damage regime there simply is no strong variation in detachment times and diffusion is the main factor. Stronger variation in detachment times would be rather expected in the regime between controlled formation damage and high salinity.

In summary, a total of 34 experiments have been conducted, of which the first 14 experiments were used to test the setup and establish protocols. Of the remaining 20 experiments, 5 showed the low salinity effect. The remaining 15 experiments that failed was due to detachment of the droplets during high salinity, or due to an absence of significant contact angle change during low salinity. These were caused by the large variation in substrate preparation and oil deposition protocols. For the future, it is therefore recommended to improve the experimental protocols, in particular the optical resolution of the contact angle measurement, and to automate and parallelize the data processing to gather larger data series for better statistics. Also the oil detachment should be treated on a more theoretical basis with the aid of numerical modeling, to explore the potential of this experimental model system for low salinity waterflooding.

6. References

- [01] "Huligan0". "*Drawing of an oil reservoir anticline trap*". An active contributor for Wikipedia.org.
- [02] Ligthelm, D. (2009). "Novel Waterflooding Strategy by Manipulation of Injection Brine Composition". *SPE 119835*.
- [03] Prof. Glover, A. "*Opportunities for CO₂ Storage around Scotland – an integrated strategic study*". Scottish Centre for Carbon Storage.
- [04] De Gennes, P. (1985). "Wetting: statics and dynamics". In *Reviews of Modern Physics* (pp. 827–863).
- [05] Buckley, J. S. (n.d.). "Fundamentals of Wettability". *New Mexico Petroleum Recovery Research Center*.
- [06] Dr. Kopeliovich, D. (n.d.). "*Stabilization of colloids*". Retrieved from SubsTech: www.substech.com
- [07] Tang, M., & Morrow, N. (1996). "Effect of temperature, salinity and oil composition on wetting behavior and oil recovery by waterflooding". *Society for Petroleum Engineering (SPE)*.
- [08] Lager, A. (2008). "Low Salinity Oil Recovery - An Experimental Investigation". *PetroPhysics*.
- [09] Ligthelm, D. (2009). "Novel waterflooding strategy by manipulation of injection brine composition". *SPE 119835*.
- [10] maker_unknown. (n.d.). "Contact angle of a liquid droplet wetted to a rigid solid surface.". *Licensed under Wikipedia Commons*.
- [12] Lager, A. (2008). "Low salinity oil recovery—an experimental investigation". *PetroPhysics 957579*.
- [13] Tang, M., & Morrow, N. (1999). "Influence of brine composition and fines migration on crude oil brine rock interactions and oil recovery". *Journal of Petroleum Science & Engineering*, 99-111.
- [14] Austad, T. (2010). "Chemical mechanism of low salinity water flooding in sandstone reservoirs". *SPE 129767*.
- [15] 'Larryisgood'. (n.d.). "A diagram of an electrical double layer". *an active contributor to Wikipedia.org*.
- [15] Cense, A. W., Berg, S., Jansen, E., & Bakker, K. (2011). "Direct visualization of designed water flooding in model experiments" by , SPE 144936, De Haagse Hogeschool. *SPE 144936*.
- [16] Menzel-Gläser. *dimensions: 26 mm by 76 mm by 1 mm*. thermo scientific microscope slide.
- [17] Jansen, E. W. (2008). "*Low Salinity Flooding: Model experiments on flat substrates, page 45*". TH Rijswijk & Shell Rijswijk.
- [18] webmaster@clays.org. (n.d.). *Clay Mineral Society*. Retrieved from Clay Mineral Society: <http://www.clays.org/SOURCE%20CLAYS/SCdata.html>
- [19] Deegan, R. D. (1997). "Capillary flow as the cause of ring stains from dried liquid drops". *Nature, Bibliography Code: 1997Natur.389..827D*.
- [20] O'Connell, J. P. (n.d.). "Diffusion in Electrolyte Solutions chapter" 11.13. In "*The Properties of Gases and Liquids*".
- [21] Bear, J. (n.d.). In "*Dynamics of Fluids in Porous Media*" (p. 627).

Appendix 1. Oil and brine properties

Table A1.1: Density of Brent crude oil as a function of temperature

T [°C]	ρ [10^3 kg/m ³]
$\pm 0,01$	$\pm 0,0005 \cdot 10^3$ kg/m ³
18	0,84719
19	0,84656
20	0,84584
21	0,84510
22	0,84436
23	0,84362
24	0,84290
25	0,84219

The density of the oil as a function of temperature in table A1.1 is plotted in figure A1.1,

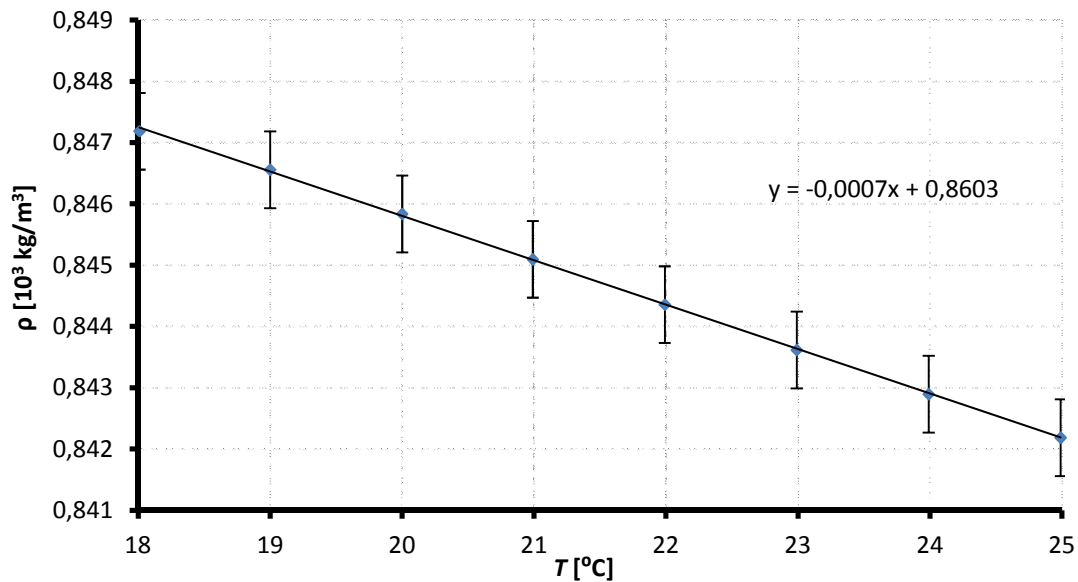


Figure A1.1: Density of Brent crude oil as a function of temperature.

The densities of the brines that were used during the experiments are presented in Table A.12. and plotted in figure A1.2.

Table A1.2: Density of the used brines as function of temperature

	Regular Morrow	¹ / ₄ Morrow	¹ / ₈ Morrow	¹ / ₁₆ Morrow
T [°C]	ρ [10^3 kg/m ³]			
$\pm 0,02$	$\pm 0,0005 \cdot 10^3$ kg/m ³			
18	1,01662	1,00382	1,00160	1,00056
19	1,01640	1,00363	1,00141	1,00037
20	1,01617	1,00342	1,00121	1,00017
21	1,01593	1,00320	1,00099	0,99996
22	1,01567	1,00297	1,00077	0,99974
23	1,01541	1,00274	1,00054	0,99951
24	1,01515	1,00249	1,00030	0,99927
25	1,01486	1,00224	1,00005	0,99902

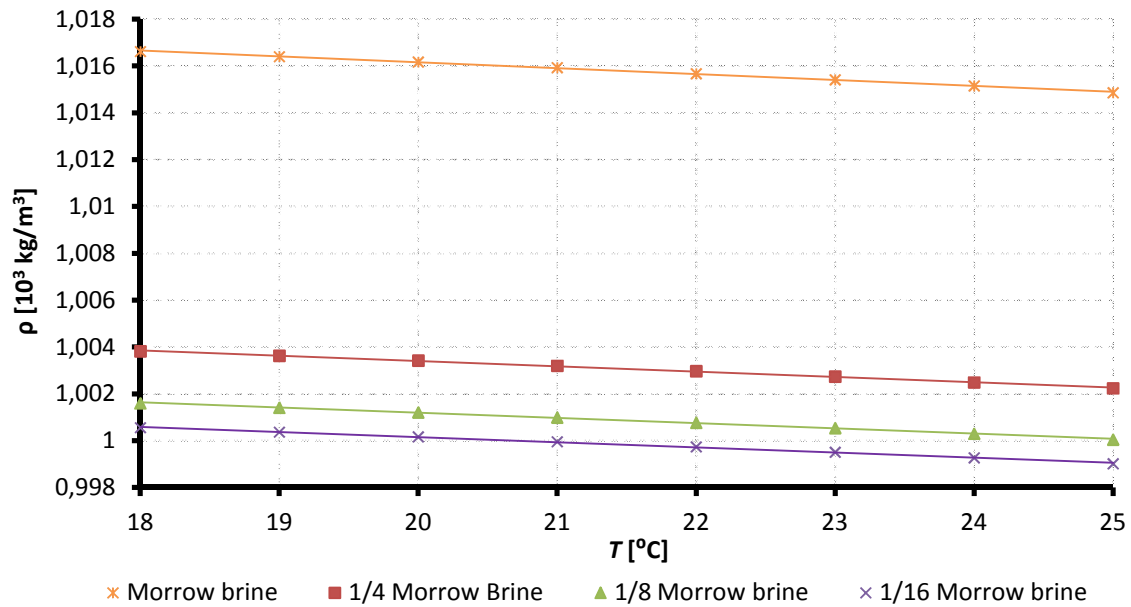


Figure A.1.2: Density of the used brines as a function of temperature.

The formulas of the trendlines in figure A.1.2 are presented in table A.1.3, so that the density of the brines can be calculated for any given temperature.

Table A1.3: Formulas of the trendlines from figure A.1.2, with the margin of error

Brine Composition	Formula of trendline
Morrow	$\rho = (1,0212 \pm 0,0003) - (0,00025 \pm 0,00002)T$
¹ / ₄ Morrow	$\rho = (1,0079 \pm 0,0003) - (0,00023 \pm 0,00002)T$
¹ / ₈ Morrow	$\rho = (1,0056 \pm 0,0003) - (0,00022 \pm 0,00002)T$
¹ / ₁₆ Morrow	$\rho = (1,0046 \pm 0,0003) - (0,00022 \pm 0,00002)T$

Appendix 2. Further investigation of clay concentrations

The glass slides, with the clay substrates and oil on it, are placed in a *Petri dish* that contained high saline (morrow brine) water. In figure A2-1 an example of a used *Petri dish* is shown.



Figure A2-1: example of a used Petri dish.

To know under which conditions Kaolinite should be investigated in the flow chamber, a half dozen experiments in *Petri dishes* have been performed, in which the clay patch concentration was varied from 100 mg/l, 300 mg/l, 500 mg/l, 700 mg/l, 900 mg/l and 1100 mg/l.

These *Petri dish* experiments confirmed once more that the degree of oil-wetness between the oil and clay depends heavily on the amount of clay on the glass. It turned out that the “ideal” clay patch concentration for Kaolinite is somewhere between 700 mg/l and 1100 mg/l. And for Montmorillonite the “ideal” clay patch size is somewhere between 100 mg/l and 300 mg/l, which corresponds with the previous found result of 160 mg/l.

The reason for this big difference in required clay concentration to adhere the oil to the clays, has to do with the clay properties and how the clay patch looks when the water from the clay suspension has evaporated. For instance, in figure 3.2, 4.3 and in figures A1-8 to A1-13 from appendix 1, it is clear that there is an higher clay concentration along the edges of the Montmorillonite clay patch. This particular pattern after evaporation is similar to that of a coffee stain, which is why it is often called a coffee ring.

Research ([19] Deegan, 1997) showed that this coffee ring is due to the capillary forces that try to maintain the form of the droplet. Furthermore, the different rate of evaporation alongside of the drop is able to amplify this effect. Because when water of a drop evaporates near the surface area, the capillary forces within the drop will replenish this evaporated water. And when the evaporation of water near the surface is higher than at the top, this coffee ring effect will be amplified because in this situation much more water will evaporate near the edge of the drop than in the middle. This is what essentially causes the coffee stain effect, hence the higher amount of clay near the edge of the clay patch.

But the reason why this is not observed in the Kaolinite clay patch, has probably to do with the fact that Kaolinite dissolves much less in water than Montmorillonite does. It was observed that as soon as the Kaolinite suspension was not being stirred anymore, the clays sedimented in a matter of seconds, while in the Montmorillonite suspension this was not the case. So this difference in suspending explains why there is a coffee stain effect in the Montmorillonite clay patch and there isn't one at the Kaolinite clay patch. Because when a Kaolinite suspension droplet is placed on the glass, the clay particles in the droplet sink to the glass before the water gets the chance to evaporate while the clay is homogeneously dispersed, and hence leave a coffee ring. And because Montmorillonite stays suspended much longer, it therefore does leave a coffee ring

In the figures A2-2 to A2-7, the results are shown of the Petri dish experiments for Kaolinite. In the upper left corner of every figure, the initial situation is showed before oil was placed on the clay patch and flooded in water. The bottom figure shows the situation at the beginning of the experiment, and the figure on the right is the end of the experiment (approximately 5 days later).

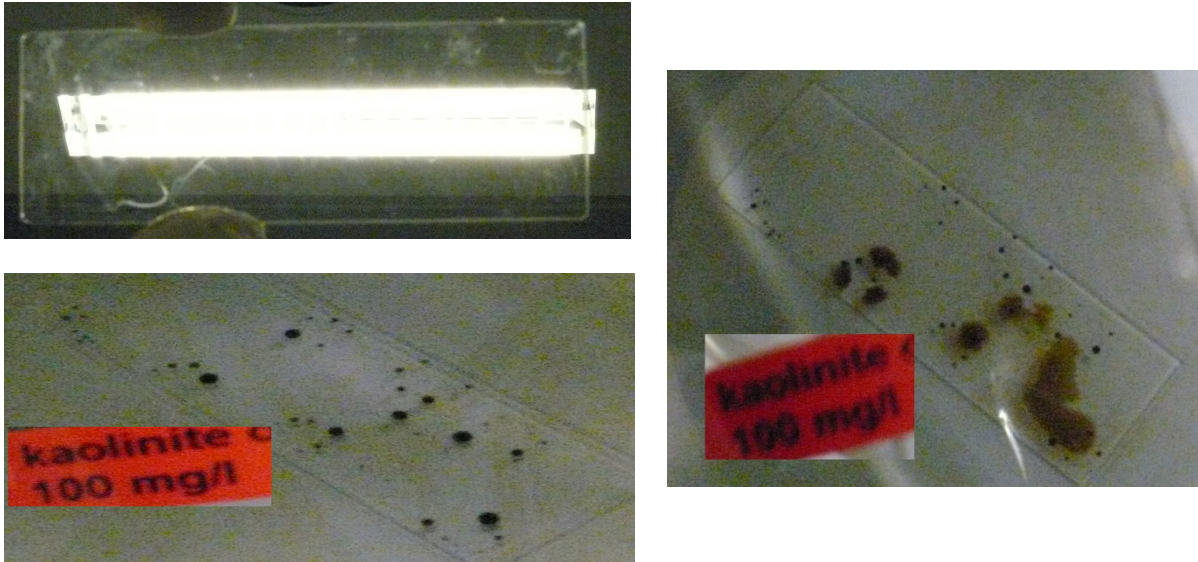


Figure A2-2: Petri dish experiment for the 100 mg/l Kaolinite clay patch. Bottom figure is start of the experiment, and the right is after approximately 5 days later. Note how in the upper left image the clay patch is barely visible due to the low clay concentration. Most of the bigger oil droplets detached, see the floating oil film in the right image.

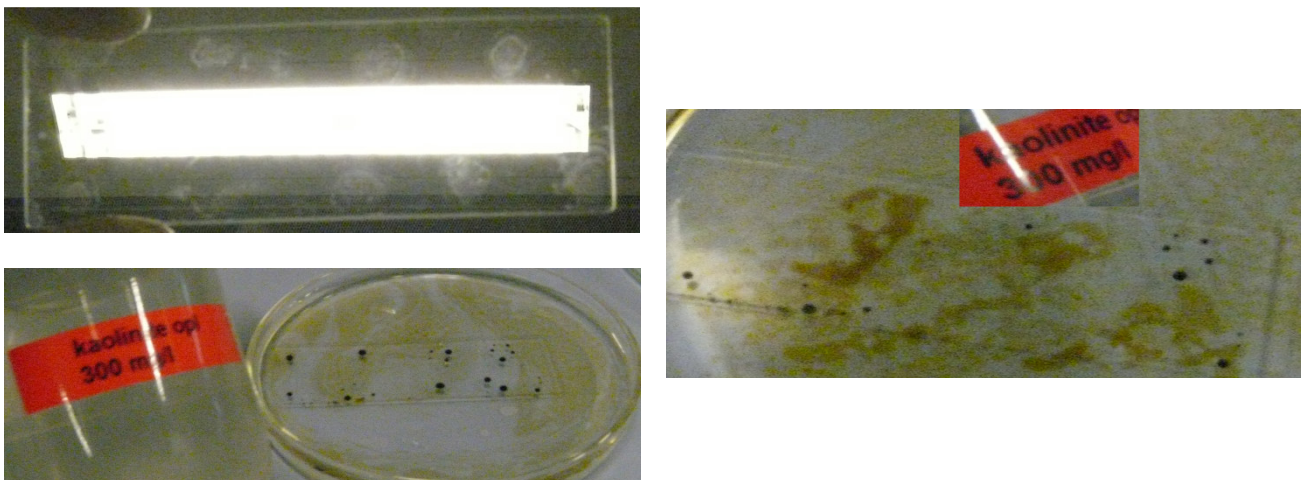


Figure A2-3: Petri dish experiment for the 300 mg/l Kaolinite clay patch. Just like for the 100 mg/l experiment, most of the droplets detached during the experiment. Note how the clay patch is now significantly better visible.

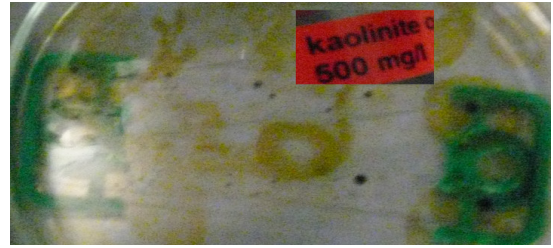
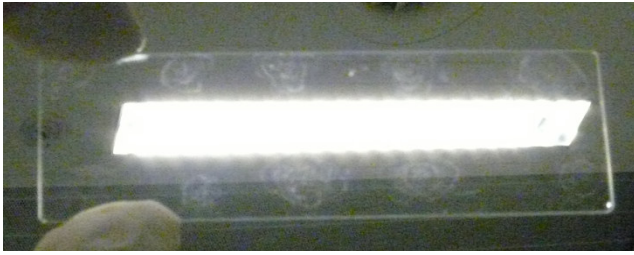


Figure A2-4: Petri dish experiment for the 500 mg/l Kaolinite clay patch. During this experiment already significantly less droplets detached.

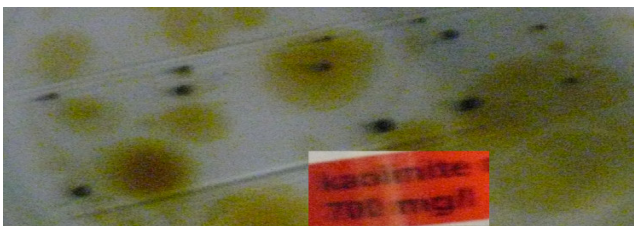


Figure A2-5: Petri dish experiment for the 700 mg/l Kaolinite clay patch. Just a few small droplets managed to detach during the experiment, while most of the oil droplets stayed connected to the clays. Note how three clay patches are “connected”, see the upper left image, due to the spreading of the placed clay suspension..



Figure A2-6: Petri dish experiment for the 900 mg/l Kaolinite clay patch. In this experiment seven droplets managed to detach, which is a great portion of the initial placed oil. This result does not correspond with the expectations. A possible explanation might be that the clay suspension was not stirred to well, because the clay patch image in the upper left is not as visible as in the 700 mg/l and 1100 mg/l experiment.

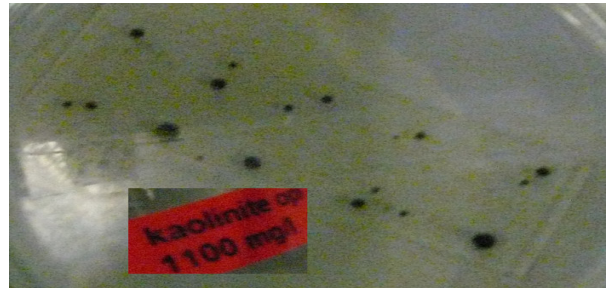
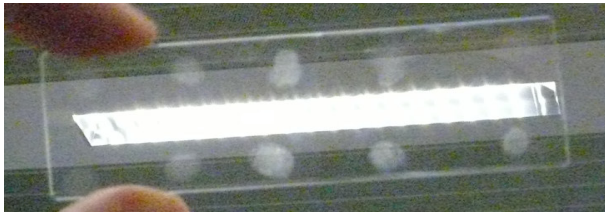


Figure A2-7: Petri dish experiment for the 1100 mg/l Kaolinite clay patch. Unlike the 900 mg/l experiment, the 1100 mg/l experiment did correspond with the expectations.

Figure A2-2 to A2-7 shows the Petri dish experiments for Kaolinite. It is clear that the clay patches of Kaolinite differ very much from Montmorillonite. The Kaolinite clay patch tends to have a much more homogeneous clay concentration, while the Montmorillonite clay patch has in all cases a higher concentration at the edges. This is also why the oil droplets in the Montmorillonite experiments are formed at the edges because that is where the adhesion is the strongest.

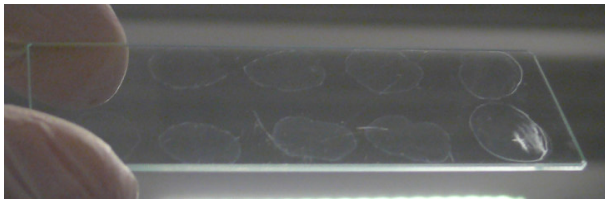


Figure A2-8: Petri dish experiment for the 100 mg/l Montmorillonite clay patch. Oil droplets detached immediately.



Figure A2-9: Petri dish experiment for the 300 mg/l Montmorillonite clay patch. No oil detachment, but the contact angle changed to a more water-wet state.

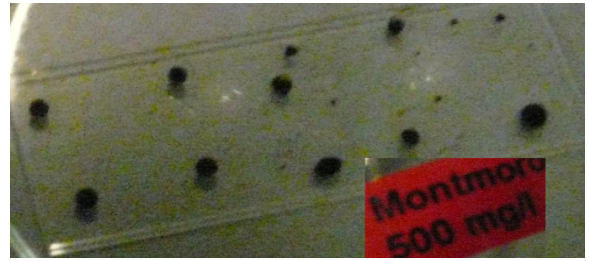
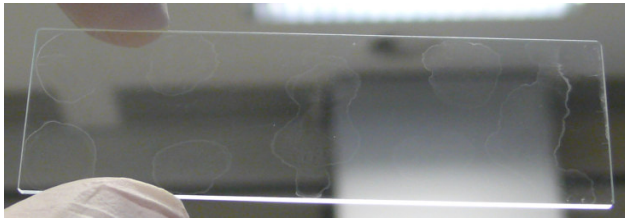


Figure A2-10: Petri dish experiment for the 500 mg/l Montmorillonite clay patch. No oil detachment, but the contact angle changed to a more water-wet state, just as in the 300 mg/l experiment.

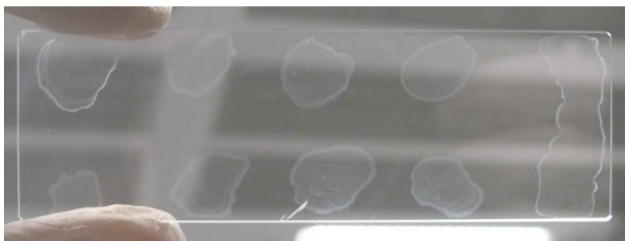


Figure A2-11: Petri dish experiment for the 700 mg/l Montmorillonite clay patch. No oil detachment once more, and less change in contact angle to a more water-wet state.

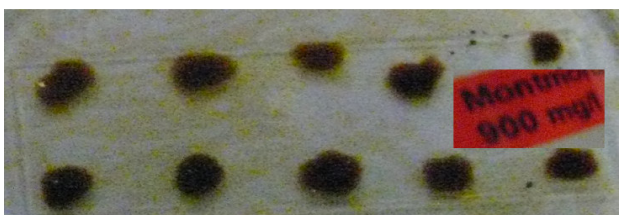
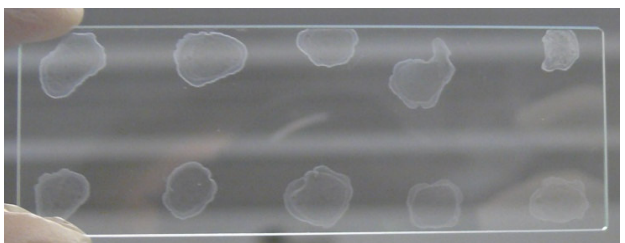


Figure A2-12: Petri dish experiment for the 900 mg/l Montmorillonite clay patch. Very little significant change in contact angle, while one droplet managed to detach. Aside from speculation, no rational explanation could have been found for this.

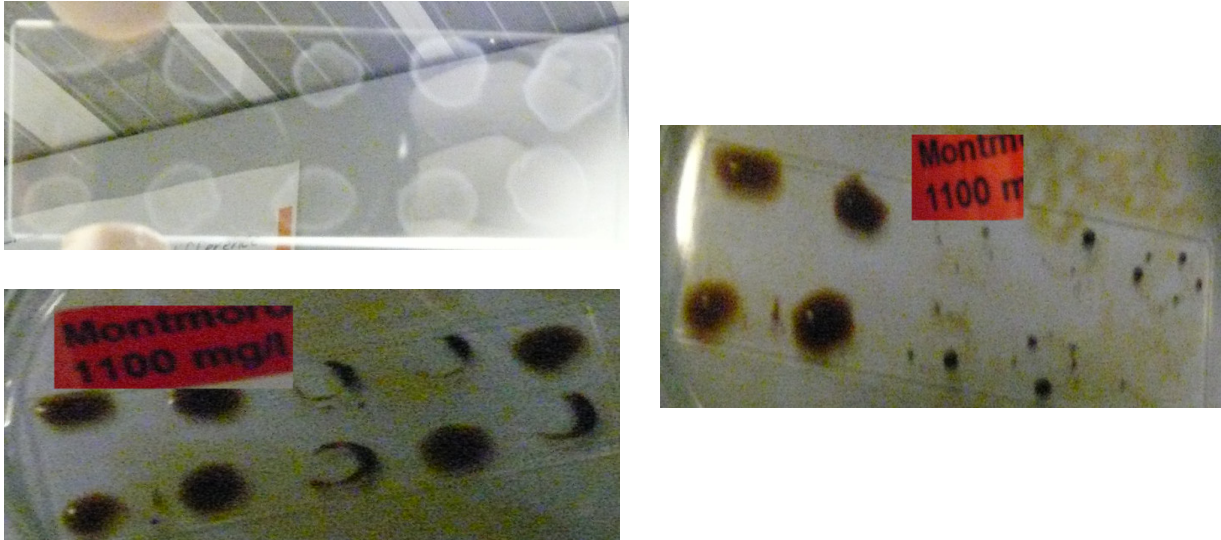


Figure A2-13: Petri dish experiment for the 1100 mg/l Montmorillonite clay patch. Very little significant change in contact angle, while two droplets managed to detach. Aside from speculation, no rational explanation could have been found for this.

Aside from couple exceptions, it is clear that the force between the oil and clay becomes stronger when the clay concentrations increases. This is observed through a consistently less change in contact angle when the clay concentrations is increased. It is therefore important that the concentration of the clay suspension is not too high, because otherwise it will become more difficult to study the low salinity effect.

For Montmorillonite the best clay concentration turned out to be somewhere between 100 mg/l and 300 mg/l, which corresponds with the initially found result by trial and error, see §4.1. And Kaolinite, which has not been investigated before, has an “ideal” clay patch size somewhere between 700 mg/l and 1100 mg/l.

Appendix 3. Overview of the experiments

This chapter gives an overview of all the performed experiments and analyzed data. Unfortunately not all the data could be presented in the main report due to the fact that not all the data was equally useful or in line of research. Nevertheless, this data is for good measure also presented below. This includes:

- Contact angle change as a function of time/salinity for the droplets that were excluded from the main results in chapter 4
- Contact area change as a function of time/salinity for the droplets that were excluded from the main results in chapter 4
- Dimensionless times, diffusion times and τ 's of all the droplets

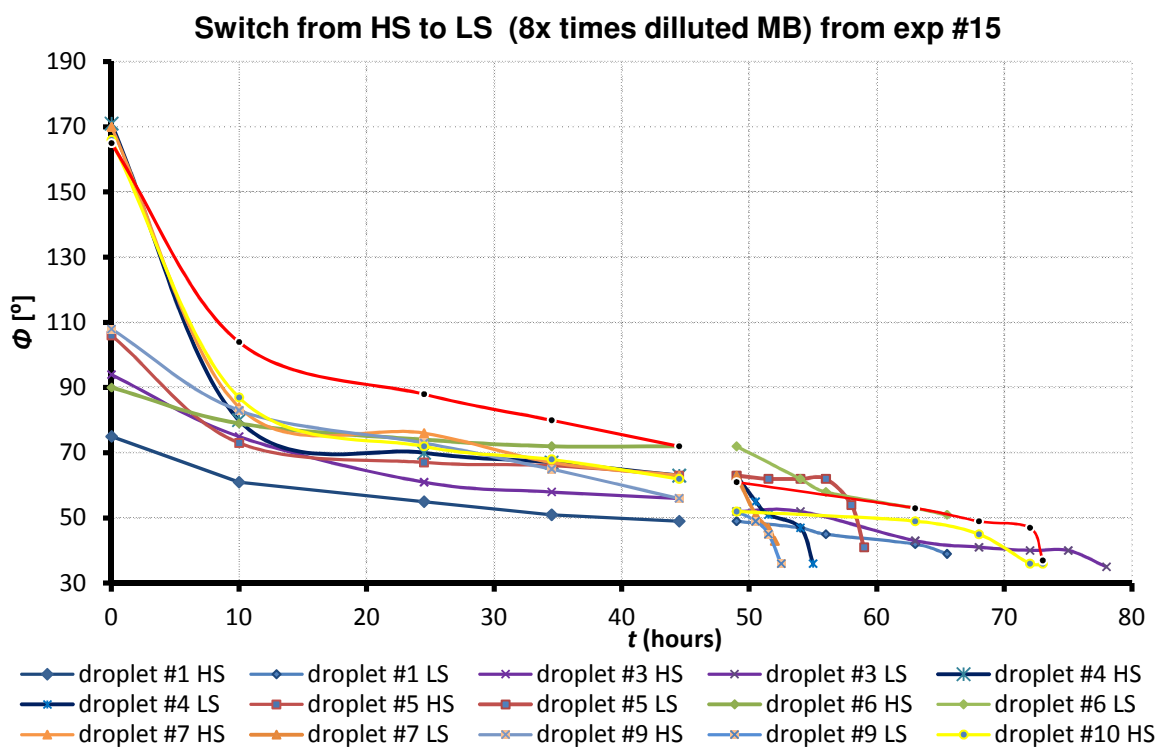


Figure A3.1: Contact angle change is plotted as a function of time for all the droplets.

Switch from HS to LS (8x diluted Morrow brine) from exp #17

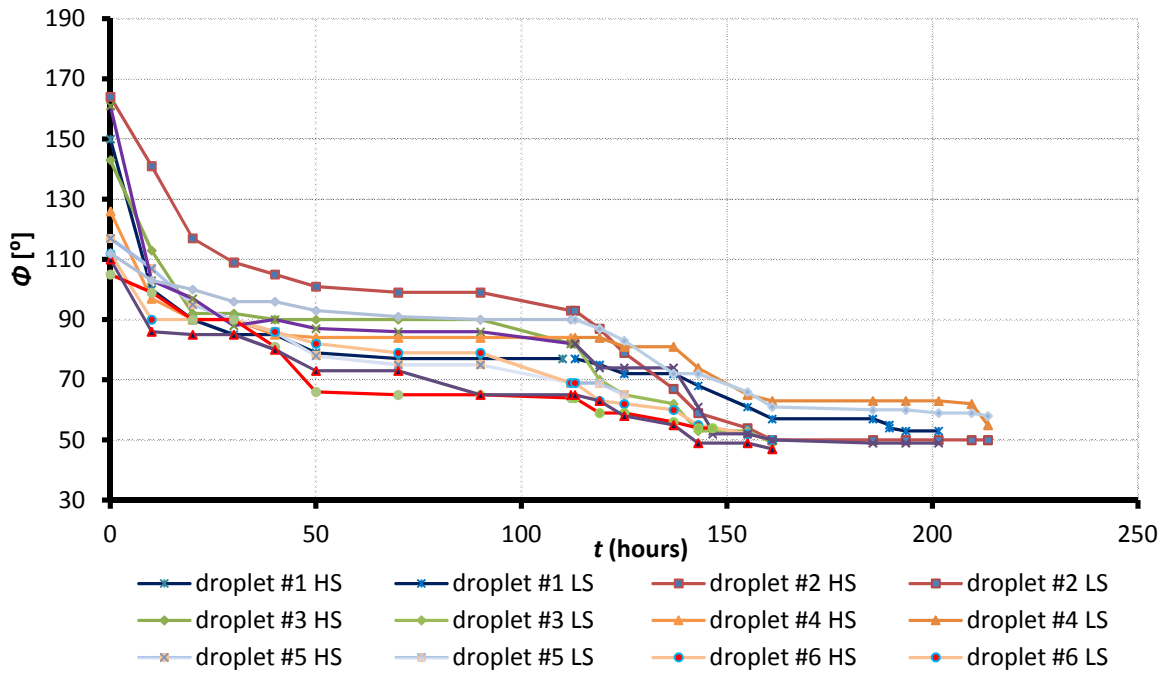


Figure A3.2a: Contact angle change is plotted as a function of time for all the droplets.

$D_{contact\ area}$ as a function of time and salinity (8x diluted exp #17)

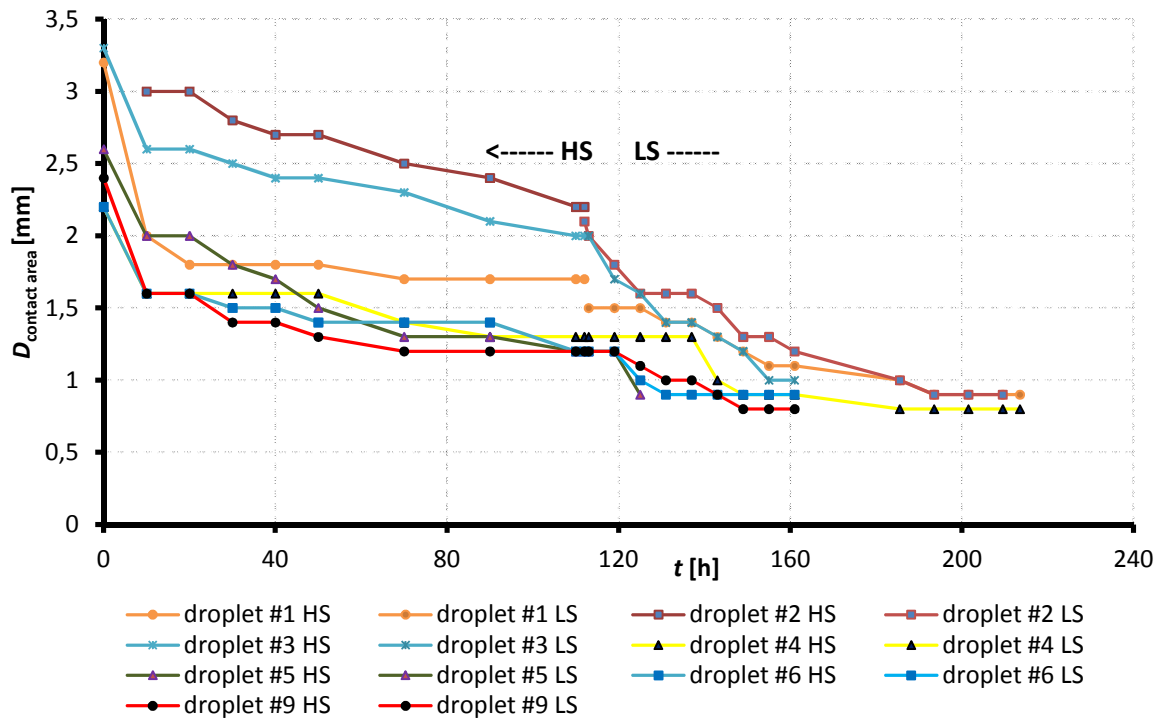


Figure A3.2b: The change in diameter of the contact area between of all the droplets plotted as a function of time for experiment #17 when it was exposed to 8x diluted Morrow brine low saline water.

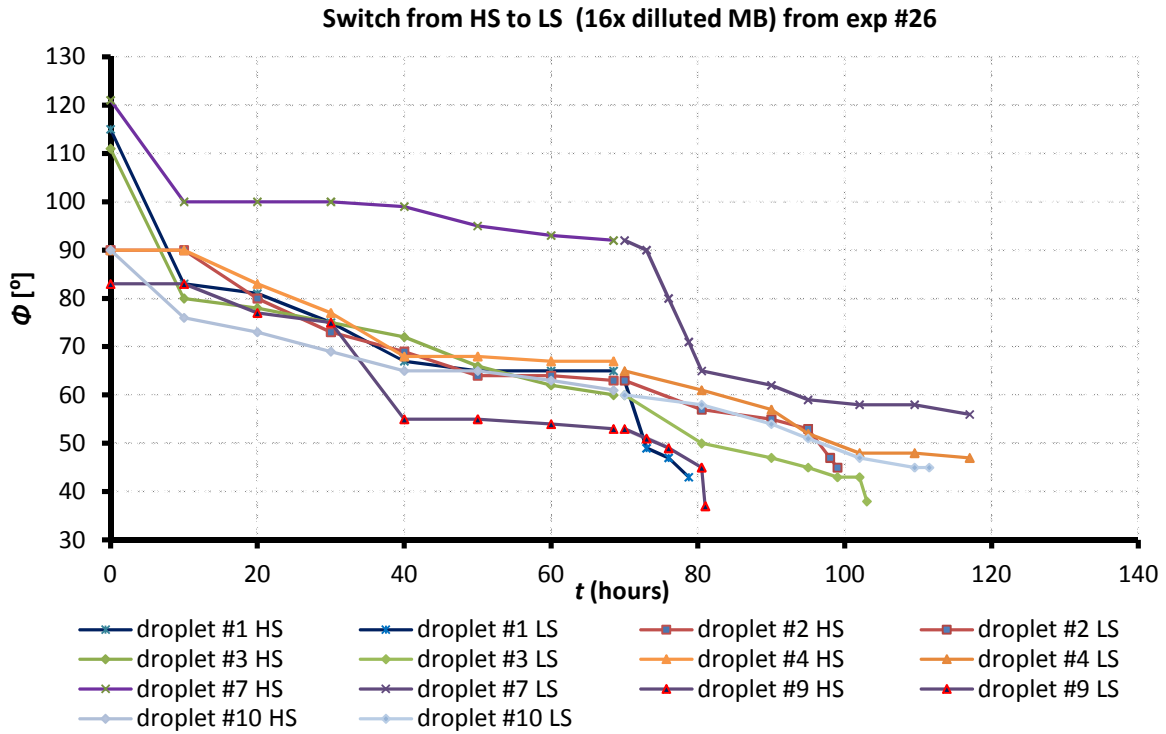


Figure A3.3: Contact angle change is plotted as a function of time for all the droplets.

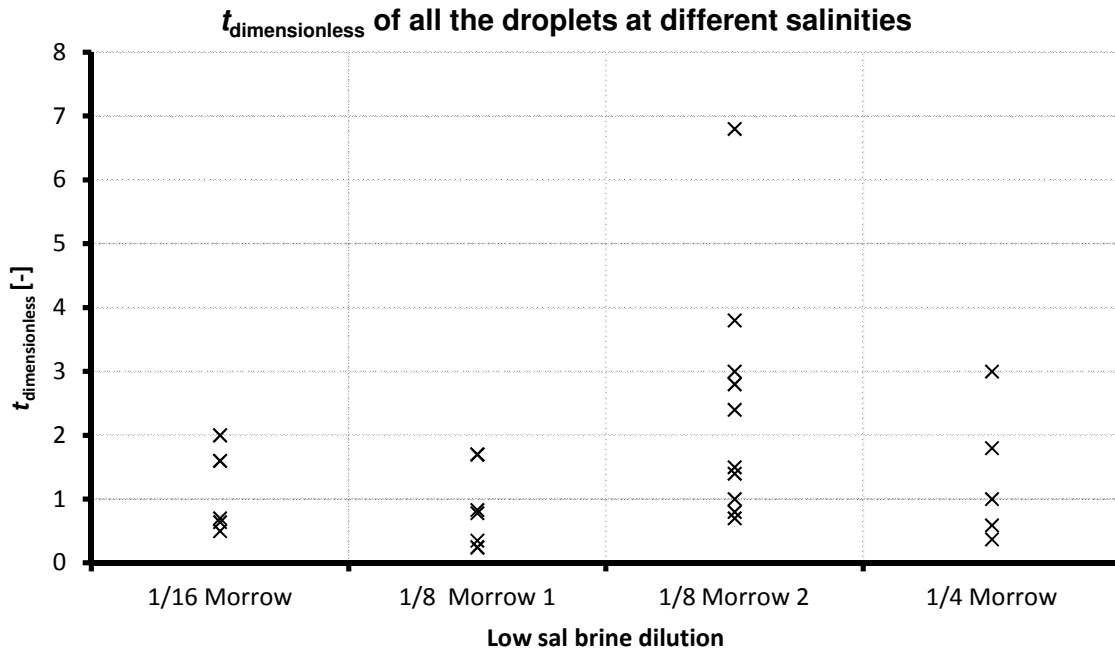


Figure A3.4: Plotted dimensionless time as a function of the brine dilution, for all the droplets that responded to the low salinity water. Respectively, $1/16$ Morrow is experiment #26, $1/8$ Morrow 1 is experiment #17, $1/8$ Morrow 2 is experiment #15 and $1/4$ Morrow is experiment #20.

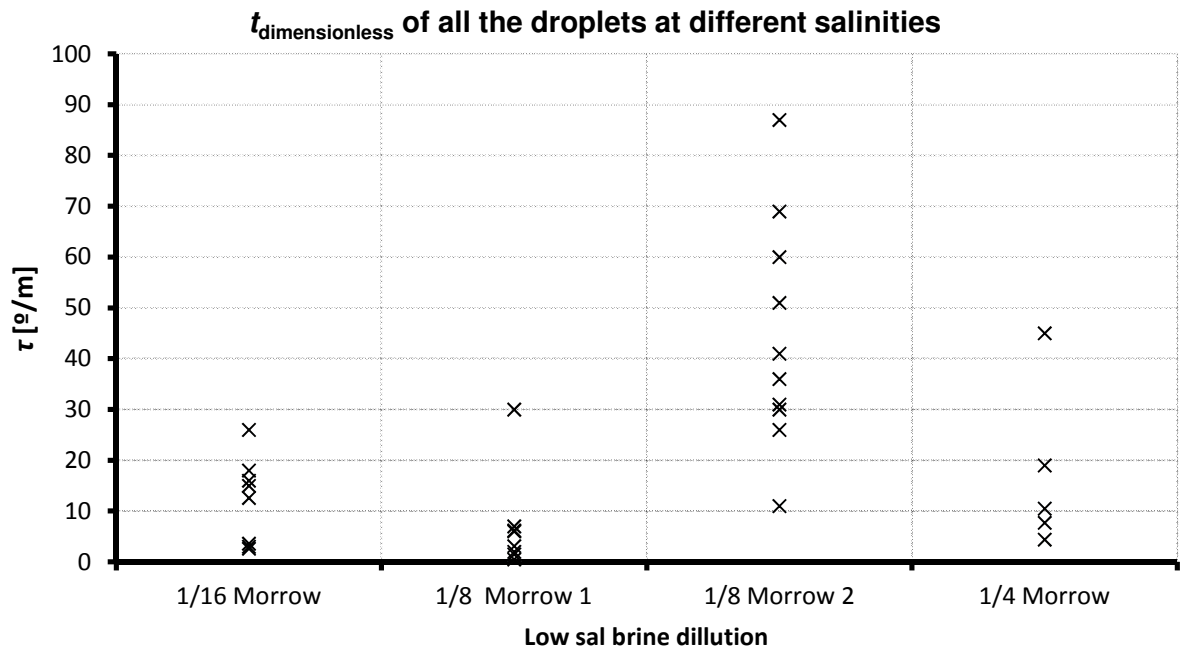


Figure A3.5: Plotted τ as a function of brine dilution for all the droplets that responded to the low salinity water. Respectively, $1/16$ Morrow is experiment #26, $1/8$ Morrow 1 is experiment #17, $1/8$ Morrow 2 is experiment #15 and $1/4$ Morrow is experiment #20.